UNIVERSIDADE DE SÃO PAULO
FACULDADE DE ODONTOLOGIA DE BAURU

LETICIA FLORINDO PEREIRA

Experimental calcium phosphate ceramic with titanium dioxide nanoparticles: manufacturing, characterization, mechanical and chemical properties analysis

Cerâmica experimental a base de fosfato de cálcio com adição de nanopartículas de dióxido de titânio: desenvolvimento, caracterização e análise de propriedades mecânicas e química

BAURU
2022

LETÍCIA FLORINDO PEREIRA

Experimental calcium phosphate ceramic with titanium dioxide nanoparticles: manufacturing, characterization, mechanical and chemical properties analysis

Cerâmica experimental a base de fosfato de cálcio com adição de nanopartículas de dióxido de titânio: desenvolvimento, caracterização e análise de propriedades mecânicas e química

Dissertação constituída por artigo apresentada à Faculdade de Odontologia de Bauru da Universidade de São Paulo para obtenção do título de Mestre em Ciências no Programa de Ciências Odontológicas Aplicadas, na área de concentração Reabilitação Oral.

Orientadora: Profa. Dra. Ana Flávia Sanches Borges

BAURU
2022

Pereira, Letícia Florindo
Experimental calcium phosphate ceramic with titanium dioxide nanoparticles: manufacturing, characterization, mechanical and chemical properties analysis / Letícia Florindo Pereira. -- Bauru, 2022.
48 p. : il. ; 31 cm.

Dissertação (mestrado) -- Faculdade de Odontologia de Bauru, Universidade de São Paulo, 2022.

Orientadora: Profª. Drª. Ana Flávia Sanches Borges

ERRATA

FOLHA DE APROVAÇÃO

DEDICATÓRIA

Aos meus pais Jason e Márcia e à minha irmã Leda.

Porque o amor pela minha família é o que me renova e abastece o meu coração. A vocês dedico não somente essa, mas todas as realizações da minha vida.

AGRADECIMENTOS

Agradeço primeiramente a **Deus**, pelo Seu infinito amor, por estar sempre comigo e por preencher a minha vida. Que os meus sonhos continuem alinhados com os dEle.

Ao meu pai, **Jason César Brega Pereira**, que é o meu exemplo de caráter, de dedicação e quem me ensinou a nunca desistir. Quantas foram as vezes que eu iniciei um projeto e pensei em desistir, mas ele nunca deixou. E, após concluir esses projetos, o sentimento sempre foi o mesmo: valeu a pena e foi maravilhoso. Muito obrigada pai, por me ensinar a ser persistente. Hoje sei perfeitamente que, se posso desfrutar do privilégio de realizar e viver um sonho meu é graças a você.

À minha mãe, **Márcia Jampaulo Florindo Pereira**, meu exemplo de bondade, leveza e fé. Em quem eu me espelhei para cursar Odontologia. Sempre me coloca pra cima com seu alto astral. Tem o dom de colorir o mundo e tornar tudo mais divertido. Você sempre fez dos meus sonhos, os seus. Não consigo encontrar palavras para agradecer todo seu amor. Só desejo que sinta o meu amor e gratidão.

À minha irmã, **Leda Florindo Pereira**, minha confidente e melhor amiga. Obrigada por estar sempre ao meu lado. Você é essencial em minha vida e faz do meu mundo um lugar mais leve.

À minha orientadora, **Profa. Dra. Ana Flávia Sanches Borges**, que em momento algum mediu esforços para a realização desse meu sonho. Te agradeço por toda ajuda e ensinamentos transmitidos. Especialmente, por sempre me motivar, incentivar e por confiar em mim, desde a minha Graduação até o Mestrado. Agradeço todas as oportunidades que me concedeu. Ela é responsável por uma enorme contribuição no meu crescimento profissional e também pessoal. Sou admiradora da sua postura, competência e ética, e digo com toda certeza e carinho que foi uma honra ser sua orientada.

Ao doutorando **Lucas José de Azevedo Silva**, um exemplo de pós-graduando e profissional, que eu admiro e constantemente me inspira a ser como ele. Ele tira do tempo dele para ajudar os outros, e sempre faz isso feliz e com muito amor. Se entrega completamente para tudo o que se propõe a fazer. E comigo não foi diferente, me ajudou em absolutamente tudo o que eu precisei. Obrigada pela paciência, por compartilhar tantos conhecimentos e, principalmente, por se tornar um grande amigo.

À Profa. Dra. **Brunna Mota Ferrairo**, também um exemplo de pessoa e profissional. Apaixonada pela ciência e por tudo o que faz. Sempre muito leal aos dela, me ajudou com muito carinho e paciência. Me transmitiu incontáveis ensinamentos. Eu amo quando ela diz que vê um pouco dela em mim, pois a admiro tanto, e ao pensar que posso ser como ela, me sinto feliz.

Aos meus amigos e companheiros de pesquisa, **Raphaelle Santos Monteiro** e **Pedro Rodrigues Minim**, que viveram esses anos intensos de mestrado comigo. A conquista de um é a conquista do outro. Agradeço os incentivos, a parceria e o respeito que compartilhamos.

Lucas, Brunna, Rapha e Pedro, vocês, sem dúvidas, marcaram a minha história na pós-graduação, e me ensinaram que ninguém faz nada sozinho. Levarei vocês no coração por toda a vida. Sem dúvidas, os maiores presentes que eu ganhei do mestrado.

À minha prima, **Luísa Della Barba**. O que sinto por ela é amor de irmã e minha vida tem muito sentido com ela presente. Obrigada por todo apoio e segurança que me transmite, por viver as minhas aventuras como se fossem suas. Que a gente siga crescendo e evoluindo com nossas diferenças e que nosso amor uma pela outra permaneça intacto pra sempre.

Ao meu namorado, **Thales Lippi Ciantelli**, que me transmite calma e paciência como mais ninguém. Ele me fortalece, me incentiva e me inspira todos os dias, com seu jeitinho gentil e dedicado de ser. Obrigada pela nossa sintonia e amor, e que a gente siga se apoiando e admirando por toda vida.

Aos meus sogros, **Ricardo Kleiner Ciantelli** e **Laís Pedroso Lippi Ciantelli**, que são meus colegas de profissão e que desde a minha formação, me acolheram, me incentivaram e me inspiraram a praticar a Odontologia. Graças a vocês eu sou apaixonada e realizada pela profissão que escolhi trilhar. Vocês são a referência do que eu quero me tornar um dia profissionalmente.

Ao meu afilhado, **Caetano Moraes Ciantelli**, por quem eu rezo todos os dias. Ele me motiva e me ensinou um significado de amor que nunca antes havia sentido.

A todos do grupo de pesquisa TRATEBIO (*Translational Team for Biomaterials*), em especial ao **Prof. Dr. Carlos Alberto Fortulan** por ser o idealizador e precursor deste trabalho e sempre nos receber de braços abertos. E **Prof. Dr. Paulo Noronha Lisboa Filho**, por toda paciência e os muitos ensinamentos transmitidos. Sempre estiveram à disposição para me ajudar e sanar minhas dúvidas. Através desse grupo eu aprendi o valor da interdisciplinaridade. O quanto a contribuição de diferentes áreas é capaz de transformar e enriquecer uma pesquisa. Ainda mais quando se tem amor e comprometimento com o que se faz.

Um agradecimento especial aos professores doutores **David Santos Souza Padovini** e **Celso Antonio Goulart**, que foram sempre muito generosos e atenciosos comigo e me ajudaram em todos os momentos que eu precisei.

Ao Prof. Dr. **Paulo Afonso Silveira Francisconi**, nosso querido “Paulinho”. Um professor exemplar. Que esbanja carinho e simpatia por onde passa. Obrigada pelo apoio, tranquilidade e motivação que me transmitiu em todos esses anos.

À Profa. Dra. **Simone Soares**, por quem, na Graduação, eu não tive o privilégio de me aproximar, pelo azar do desencontro, mas fui recompensada na Pós-Graduação. Ela me surpreendeu com seu cuidado, atenção e capricho. Foi um privilégio acompanha-la nas clínicas e aprender tanto. Obrigada por compartilhar seus conhecimentos comigo e por tornar nossas quartas-feiras a tarde sempre mais alegres.

Ao querido técnico **Alcides Urias da Costa**. Pelo convívio alegre e amigável no departamento de Materiais Dentários. Sempre disposto a ajudar e incentivar. Sempre muito atencioso e feliz. Faz o melhor café de toda a Faculdade. Sentirei saudades e te levo no coração.

À **Faculdade de Odontologia de Bauru da Universidade de São Paulo** (FOB-USP). Minha casa desde 2014, quando ingressei na Graduação. Essa instituição transformou a minha vida. Hoje sei reconhecer os privilégios que tive. Os melhores professores, funcionários prestativos e atenciosos, uma estrutura sem igual, oportunidade de desenvolvimento científico, atendimento odontológico de qualidade a quem precisa, entre muitas outras coisas. O sentimento de orgulho e gratidão por essa instituição que sempre me acolheu é inexplicável.

Ao **Departamento de Prótese da FOB-USP**, representado pela chefe Profa. Dra. **Ana Lúcia Pompéia Fraga de Almeida**, junto aos professores doutores **Estevam Augusto Bonfante**, **José Henrique Rubo**, **Karin Hermana Neppelenbroek**, **Paulo César Conti**, **Pedro César Garcia de Oliveira**, **Renato de Freitas** e **Vinícius Carvalho Porto**. Agradeço por compartilharem seus conhecimentos e admiro o amor com que se dedicam constantemente ao que fazem.

Aos **Departamentos de Física da Universidade Estadual Paulista Júlio de Mesquita Filho (UNESP Bauru)**, **de Engenharia Mecânica e de Materiais da USP São Carlos**, à **Faculdade UNICAMP campus Piracicaba** e **Faculdade de Odontologia de São Paulo (FO-USP)**, por toda a infraestrutura usufruída durante a pesquisa e oportunidade de desenvolvimento acadêmico.

Aos meus colegas de pós-graduação que ingressaram comigo no mestrado, **Amanda Maia**, **Camila Alves**, **Eliezer Gutierres**, **Gabriela Robles Mengoa**, **Karolyn Sales Fioravanti**, **Laura Catalí Ferreira Peralta**, **Maria Emilia Servín Berder**, **Mariana Miranda de Toledo Piza**, **Matheus Souza Campos Costa**, **Sandy Maria da Silva Costa** e **Tatiana Prosini da Fonte**. Obrigada pela troca de experiências, companhia e parceria que tivemos nesses anos. Com certeza, cada um de vocês contribuiu para o meu crescimento pessoal e profissional, vocês são exemplos de dedicação e torço muito pelo sucesso de cada um.

Às minhas amigas **Amanda Gomes**, **Amanda Braga**, **Amanda Papoti**, **Ana Luiza Panini**, **Ananda Vicentini**, **Angela Taranto**, **Lívia Fabbro** e **Verônica Corradini**. Todas passamos por muitas mudanças, aprendizados, crescimento pessoal, profissional, cada uma indo atrás de suas conquistas e sonhos. E não importa o quanto tudo mude de lugar, nossa amizade permanece intacta. Obrigada por acompanharem essa jornada comigo, apoiando e vibrando sempre. Amo vocês.

À **Coordenação de Aperfeiçoamento de Pessoal de Nível Superior (CAPES)** – Código de Financiamento 001 – pela concessão da bolsa de estudos do Mestrado, auxílio indispensável para a realização deste trabalho.

Aos **professores integrantes da banca examinadora**, por terem dedicado seu tempo analisando e contribuindo para o aperfeiçoamento deste trabalho.

A todos que de alguma forma colaboraram direta ou indiretamente para que essa etapa tão importante da minha vida fosse concluída, o meu sincero agradecimento.

"Só é possível caminhar em direção a excelência se
você souber que não sabe algumas coisas."

Mario Sergio Cortella

ABSTRACT

Experimental calcium phosphate ceramic with titanium dioxide nanoparticles: manufacturing, characterization, mechanical and chemical properties analysis

The following study proposed the development and characterization of a new ceramic for dental use made from hydroxyapatite (HA) extracted from bovine bones, with the intention of reusing these solid wastes and turning them into a sustainable and low-cost material. Furthermore, the addition of titanium dioxide (TiO_2) nanoparticles to this material was carried out in an attempt to improve its mechanical and chemical properties. Disks (Ø = 14 ± 2 mm; thickness = 1.2 ± 0.2 mm) were obtained through uniaxial and isostatic pressing from bovine hydroxyapatite powder and TiO_2 nanoparticles and sintered at 1300ºC for 2 hours. Three experimental groups were developed (HA, HA+5%TiO_2 and HA+8%TiO_2) and microstructurally characterized by X-ray diffraction (XRD), scanning electron microscopy (SEM) and energy dispersive spectroscopy (EDS). For mechanical and chemical analysis, indentation fracture (IF), biaxial flexural strength (BFS) and chemical solubility tests were performed. XRD spectra revealed the appearance of a peak corresponding to b-tricalcium phosphate (ß-TCP) for HA group. For HA+5%TiO_2 and HA+8%TiO_2, the entire composition was converted into ß-TCP and calcium titanate ($CaTiO_3$). IF toughness was higher for HA+5%TiO_2 (1.34 ± 0.26 MPa.$m^{1/2}$) and HA+8%TiO_2 (1.28 ± 0.21 MPa.$m^{1/2}$) than for HA (0.65 ± 0.10 MPa.$m^{1/2}$). HA showed significantly higher characteristic stress (295.8 MPa) in relation to groups with 5% (235.1 MPa) and 8% (214.4 MPa) TiO_2 nanoparticles. The Weibull modulus values of the three groups were statistically similar. The solubility results indicated that all experimental ceramics were above the 2000 ug/cm^2 limit set by the International Organization for Standardization (ISO) 6872:2015. The experimental calcium phosphate ceramic with additions of 5% and 8% of TiO_2 achieved desirable mechanical properties, but very high chemical solubility values.

Keywords: Ceramics. Dental Materials. Bone. Nanotechnology. Apatites.

RESUMO

Este estudo propôs o desenvolvimento e caracterização de uma nova cerâmica para uso odontológico feita a partir de hidroxiapatita (HA). A HA foi extraída de ossos bovinos, com a intenção de reaproveitar esses resíduos sólidos e transformá-los em um material sustentável e de baixo custo. Além disso, a adição de nanopartículas de dióxido de titânio (TiO_2) (5 e 8%) a este material foi realizada na tentativa de melhorar suas propriedades mecânicas e químicas. Discos (Ø 14 ± 2 mm; espessura = 1.2 ± 0.2 mm) foram obtidos por prensagem uniaxial e isostática a partir de um pó de hidroxiapatita bovina e nanopartículas de TiO_2 e sinterizados a 1300ºC por 2 horas. Três grupos experimentais foram desenvolvidos (HA, HA+5%TiO_2 e HA+8%TiO_2) e caracterizados microestruturalmente por difração de raios-X (DRX), microscopia eletrônica de varredura (MEV) e espectroscopia por energia dispersiva (EDS). Para análise mecânica e química dos materiais, os testes de tenacidade à fratura pelo método da indentação, de resistência à flexão biaxial (RFB) e de solubilidade química foram realizados. Os espectros de DRX revelaram, para o grupo HA, o aparecimento de um pico correspondente ao beta-tricálcio fosfato (ß-TCP). Para HA+5%TiO_2 e HA+8%TiO_2, toda a composição de HA e TiO_2 foi convertida em ß-TCP e titanato de cálcio ($CaTiO_3$). A tenacidade à fratura foi maior para HA+5%TiO_2 (1,34 ± 0,26 MPa.$m^{1/2}$) e HA+8%TiO_2 (1,28 ± 0,21 MPa.$m^{1/2}$) do que para HA (0,65 ± 0,10 MPa.$m^{1/2}$). HA apresentou resistência característica significativamente maior (295,8 MPa) em relação aos grupos com 5% (235,1 MPa) e 8% (214,4 MPa) de nanopartículas de TiO_2. Os valores de módulo Weibull dos três grupos foram estatisticamente semelhantes. Os resultados de solubilidade indicaram que todas as cerâmicas experimentais estavam acima do limite de 2000 ug/cm^2 permitido pela *International Organization for Standardization* (ISO) 6872:2015. A cerâmica experimental de fosfato de cálcio com adições de 5% e 8% de TiO_2 alcançou propriedades mecânicas desejáveis, mas valores de solubilidade química muito elevados.

Palavras-chave: Cerâmicas. Materiais Dentários. Osso. Nanotecnologia. Apatitas.

SUMÁRIO

1 **INTRODUÇÃO** 14

2 **ARTIGO** 16

3 **REFERÊNCIAS** 46

1 INTRODUÇÃO

Cerâmicas de fosfato de cálcio são estudadas para aplicações na área da saúde já há muitos anos, devido suas excelentes propriedades biológicas (MONROE *et al.*, 1971). Existem várias cerâmicas de fosfato de cálcio, que se diferenciam pela estequiometria (razão entre Ca e P presentes) e propriedades físico-químicas (ELIAZ; METOKI, 2017).

A hidroxiapatita (HA) é uma cerâmica de fosfato de cálcio e o principal componente mineral dos dentes e tecidos ósseos que vem sendo amplamente estudada na engenharia de tecidos para utilização como biomaterial em áreas médicas e odontológicas (SWETHA *et al.*, 2010; BORDEA *et al.*, 2020; LIM *et al.*, 2020). Esse material é de grande interesse em muitas áreas por apresentar admiráveis propriedades biológicas, como bioatividade, biocompatibilidade e alta osteocondutividade, já apresentando comprovação de segurança biológica e sendo amplamente utilizado na área de cirurgia e implantodontia para enxertia, regeneração óssea e revestimento de implantes (ELIAZ; METOKI, 2017; BORDEA *et al.*, 2020; GHIASI *et al.*, 2020). Essas propriedades somadas à possibilidade de utilização tanto na conformação porosa quanto densa, a permitem ser um material muito versátil, com múltiplas aplicações clínicas em Odontologia (PRAKASAM *et al.*, 2015; MBARKI *et al.*, 2017; PIRES *et al.*, 2020; BORDEA *et al.*, 2020).

HA pode ser extraída de fontes biológicas ou resíduos naturais, como cascas de ovos, algas marinhas, plantas, ossos animais ou escamas de peixes, o que é considerado um processo ecologicamente correto e sustentável (AKRAM *et al.*, 2014; MOHD PU'AD *et al.*, 2019; AGBEBOH *et al.*, 2020). Neste estudo, a cerâmica densa de HA tem sua origem na reutilização de ossos bovinos, sendo uma fonte acessível, renovável e inesgotável de HA para uso como matéria-prima, além de o método de extração ser economicamente viável e eficiente (JAYATHILAKAN *et al.*, 2012; KUSRINI; SONTANG, 2012; RINCÓN-LÓPEZ *et al.*, 2018).

Os materiais de cerâmica pura estão se tornando cada vez mais populares para substituir a estrutura dentária ausente (POGGIO *et al.*, 2017). Entretanto, a possível aplicação de uma cerâmica densa policristalina à base de HA como restauração é limitada por apresentar baixas propriedades mecânicas, como tenacidade à fratura e resistência à flexão (PRAKASAM *et al.*, 2015; ELIAZ; METOKI, 2017). Além disso, para uso como um material restaurador, a cerâmica de HA deve demonstrar

durabilidade no meio bucal, onde estariam constantemente sujeitas à dissolução por ataque químico neste ambiente (HAWSAWI *et al.*, 2020).

A Norma *ISO* (*International Standard Organization*) 6872 (2015) especifica os requisitos e métodos de ensaio padronizados para caracterizar e avaliar as propriedades de materiais cerâmicos odontológicos para restaurações e próteses fixas totalmente cerâmicas e metalocerâmicas. De acordo com os valores obtidos nos testes de resistência à flexão, tenacidade à fratura e solubilidade química, os materiais cerâmicos destinados para uso como próteses fixas podem ser classificados e indicados para o uso clínico específico (ISO 6872, 2015).

A fim de aprimorar o comportamento mecânico e a durabilidade de um material, a adição de nanomateriais tem sido proposta (FABER; EVANS, 1983; FATHI *et al.*, 2014; PIRES *et al.*, 2020). Nanopartículas de dióxido de titânio (TiO_2) têm se destacado na área odontológica como aditivo em materiais dentários, uma vez que são capazes de potencializar propriedades mecânicas (WETZEL *et al.*, 2006; XIA *et al.*, 2008; GHAHREMANI *et al.*, 2017) e biológicas (ELSAKA; HAMOUDA; SWAIN, 2011; SODAGAR *et al.*, 2017), além de diminuírem a solubilidade química dos materiais (FATHI *et al.*, 2014). A adição de nanopartículas de TiO_2 em uma cerâmica densa de HA bovina já foi investigada previamente por Pires *et al.* (2020) nas concentrações de 1%, 2% e 5% e foi demonstrado que a concentração de 5% teve o maior potencial para melhorar as características mecânicas do material. A HA com adição de 5% de nanopartículas de TiO_2 teve o valor de dureza Vickers médio (399.6 ± 15.31 HV) significativamente maior quando comparado à HA pura (335 ± 12.98 HV). Quanto à resistência a flexão, os valores permaneceram sem diferença estatística, mas alcançaram um valor aceitável (214,9 ± 36,4 MPa) de acordo com as exigências da norma ISO 6872:2015.

Atualmente, uma grande quantidade de materiais cerâmicos e vias de processamento estão disponíveis para serem utilizados em Odontologia na fabricação de restaurações (GRACIS *et al.*, 2015). No entanto, até hoje, não existe no mercado uma cerâmica que consiga integrar tecnologia, sustentabilidade, segurança biológica e baixo custo em um só material. Por apresentar-se como um material atrativo e promissor, torna-se necessário investigar o efeito da adição de TiO_2, em concentrações maiores que 5% em peso, na microestrutura e nas propriedades mecânicas e químicas de uma cerâmica densa de HA de origem bovina.

2 ARTIGO

The article presented in this Dissertation was written according to the *Dental Materials* instructions and guidelines for article submission.

Experimental calcium phosphate ceramic with titanium dioxide nanoparticles: manufacturing, characterization, mechanical and chemical properties analysis

Authors:

***Letícia Florindo Pereira*[1]**
leticia.florindo.pereira@usp.br

Lucas José de Azevedo Silva[1]
lucasjazevedos@usp.br

Brunna Mota Ferrairo[2]
brunna.ferrairo@usp.br

Pedro Rodrigues Minim[1]
pedro.minim@usp.br

Paulo Noronha Lisboa-Filho[3]
paulo.lisboa@unesp.br

Carlos Alberto Fortulan[4]
fortulan@usp.br

Jason Alan Griggs[5]
jgriggs@umc.edu

Ana Flávia Sanches Borges[2]
afborges@fob.usp.br

1. Department of Prosthodontics and Periodontology (or Periodontics), University of São Paulo (USP), Bauru School of Dentistry, Bauru, SP, Brazil. Alameda Dr. Octávio Pinheiro Brisolla, 9-75, Vila Universitária, 17012-901, Bauru, SP, Brazil.

2. Department of Operative Dentistry, Endodontics and Dental Materials, Bauru School of Dentistry, University of São Paulo. Alameda Dr. Octávio Pinheiro Brisolla, 9-75, Vila Universitária, 17012-901, Bauru, SP, Brazil.

3. Department of Physics, School of Sciences, São Paulo State University, Av. Engenheiro Luiz Edmundo Carrijo Coube, s/n, Vargem Limpa, 17033360 Bauru, SP, Brazil

4. Department of Mechanical Engineering, São Carlos School of Engineering, University of São Paulo, Avenida Trabalhador São-Carlense, 400, Centro, 13566-590 São Carlos, SP, Brazil

5. Department of Biomedical Materials Science, School of Dentistry, University of Mississippi Medical Center, 2500 North State Street, Room D528, 39216-4505 Jackson, MS, United States.

'Declarations of interest: none'.

ABSTRACT

Objectives. Develop a sustainable bovine hydroxyapatite dental ceramic with the addition of titanium dioxide (TiO_2) nanoparticles (5% and 8% by weight), analyzing the outcome of this addition to the microstructure, as well as its mechanical and chemical properties, in order to evaluate whether they satisfy the International Organization for Standardization (ISO) 6872:2015 for dental ceramics or not.

Methods. Disks were obtained through uniaxial and isostatic pressing from bovine hydroxyapatite powder and TiO_2 nanoparticles and sintered at 1300ºC for 2h. Three experimental groups were developed (HA, HA+5%TiO_2 and HA+8%TiO_2) and subjected to X-ray diffraction (XRD), scanning electron microscopy (SEM), energy dispersive spectroscopy (EDS), indentation fracture (IF), biaxial flexural strength (BFS) and chemical solubility test.

Results. XRD revealed, for HA group, the appearance of a peak corresponding to b-tricalcium phosphate (ß-TCP). For HA+5%TiO_2 and HA+8%TiO_2, the entire composition was converted into ß-TCP and calcium titanate ($CaTiO_3$). The SEM images showed a dense ceramic matrix and a uniform distribution of another phase in groups with TiO_2 nanoparticles. HA+5%TiO_2 (1.34 ± 0.26 MPa.$m^{1/2}$) and HA+8%TiO_2 (1.28 ± 0.21 MPa.$m^{1/2}$) showed significantly higher fracture toughness values than HA (0.65 ± 0.10 MPa.$m^{1/2}$). HA showed significantly higher characteristic stress (295.8 MPa) in comparison to groups with 5% (235.1 MPa) and 8% (214.4 MPa) TiO_2 nanoparticles. Differences were not observed between the Weibull modulus values. The solubility results indicated that all experimental ceramics were above the 2000 ug/cm^2 limit set by the ISO 6872:2015.

Significance. This study proposed the development and characterization of a new ceramic for dental use made from HA extracted from bovine bones, with the intention of reusing these solids waste and transforming them into a sustainable and low-cost material. Although the experimental calcium phosphate ceramic with additions of 5% and 8% of TiO_2 achieved desirable mechanical properties, the chemical solubility values were very high.

Keywords: Ceramics. Dental Materials. Bone. Nanotechnology. Apatites.

GRAPHICAL ABSTRACT

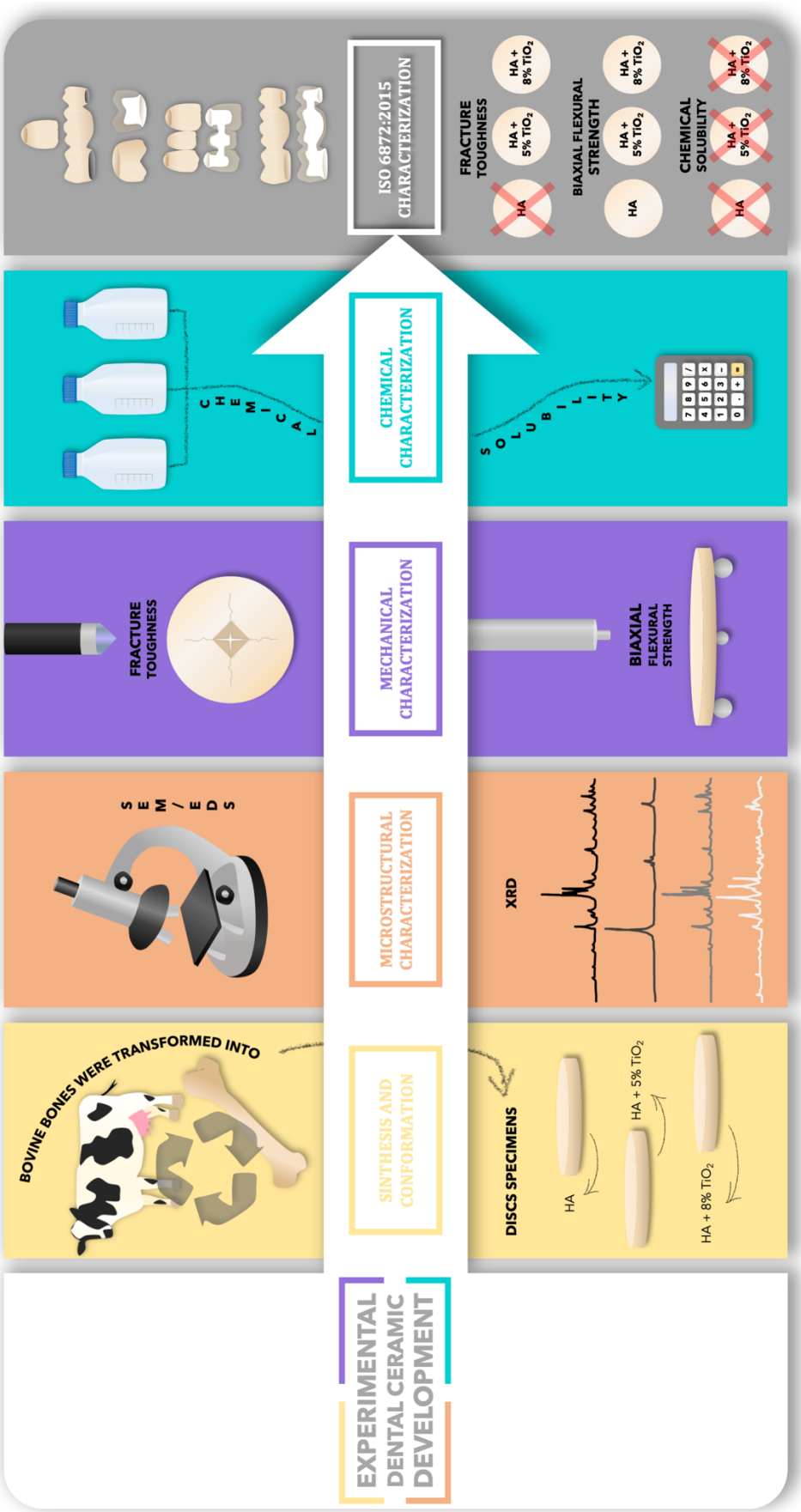

1. INTRODUCTION

Calcium phosphates (CaP) form a privileged class of biomaterials because of their remarkable biological properties [1]. Depending on the Ca/P ratio, several families of CaP can be established [2]. One of the most important CaP ceramics is hydroxyapatite (HA) (Ca/P = 1.67), the major tooth and natural bones' inorganic component [1]. HA is of great interest for many fields because of its excellent bioactivity, biocompatibility and high osteoconductivity [3]. These properties, added to the possibility of use in dense or porous conformations, allow it to be an extremely versatile material, with multiple uses in dental applications [4-7].

HA can be extracted from natural sources, such as bones from different animals [8]. HA generated from bovine bones offers economic benefits, as it relies on the use of cheap, natural and undesirable material, and is attractive from an environmental point of view, since it can be generated from waste [2]. The reuse of these solids is considered an eco-friendly, environmentally sustainable and economically viable process [9, 10].

The possibility of using a dense ceramic made from HA as a dental restoration is limited by its low mechanical properties, such as fracture toughness and flexural strength [4, 11]. Furthermore, to be used as a restorative material, HA ceramics must demonstrate durability in the oral environment, where they would be constantly subject to dissolution by chemical attack [12].

The International Organization for Standardization (ISO) 6872:2015 specifies the requirements and the corresponding testing methods to characterize and evaluate the dental ceramic materials properties for all-ceramic and metal-ceramic restorations and prostheses. According to the values obtained in the flexural strength, fracture toughness and chemical solubility tests, ceramic materials intended to be used as dental prostheses can be classified and recommended for specific clinical use [13].

In order to improve the mechanical behavior and durability of a material, the addition of nanomaterials has been proposed [6, 14, 15]. Titanium dioxide (TiO_2) nanoparticles have been getting more attention in the dental field as an additive to different materials, since they are capable of enhancing mechanical [16-18] and biological [19, 20] properties, apart from decreasing the materials' chemical solubility [15]. The addition of TiO_2 nanoparticles to a dense bovine HA ceramic has been

previously investigated [6] at concentrations of 1%, 2% and 5% and it was shown that the 5% had the greatest potential to improve its mechanical characteristics.

Currently, a large number of ceramic materials and processing methods are available to be used in the fabrication of dental restorations [21]. However, none of these integrate technology, sustainability, biological safety and low cost in a single material. The combination of HA and TiO_2 nanoparticles presents itself as an attractive and promising material and therefore, this study aims to develop a bovine hydroxyapatite dental ceramic with the addition of titanium dioxide (TiO_2) nanoparticles (5wt% and 8wt%) and investigate the outcome of this addition on the microstructure as well as on the mechanical and chemical properties, evaluating whether they satisfy the ISO 6872:2015 for dental ceramics or not.

2. MATERIAL AND METHODS

2.1. Preparation of TiO_2 nanoparticles

The TiO_2 nanoparticles were obtained by the sol–gel method. 185 mL of distilled water, 56.7 mL of isopropanol, and 2.6 mL of nitric acid (HNO_3) were added to an Erlenmeyer flask. Next, 15 mL of titanium isopropoxide (IV) were added to the solution and the contents stirred at 300 rpm for 30 min, on a magnetic plate. The solution was heated at 85 ºC while stirring. The heating and stirring patterns were maintained until the complete evaporation of the liquid, which resulted in condensation. Subsequently, the resulting gel was heat-treated at 450 ºC for two hours and reduced to a homogeneous powder (Figure 1).

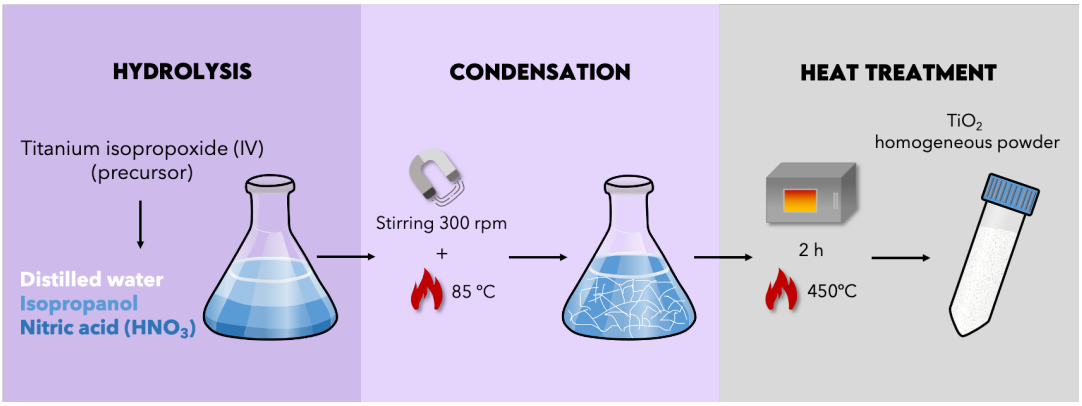

Figure 1. Flowchart of the synthesis of TiO2 nanoparticles by the sol-gel method.

2.2. Specimen preparation

Bovine metatarsus (2-year-old), which were certified to be contamination free, were collected and underwent manual, chemical (five minutes immersed in 100 vol hydrogen peroxide) and thermal (calcined at 900 °C for 24 hours) cleaning processes (Figure 2A), in order to completely remove the organic matter and kill the pathogens which may have been present.

Subsequently, the bones underwent milling processes. First manual, using a mortar and pestle (Figure 2B), and then with mills, to reduce the size of the particles and increase the reactivity among them, thus reducing the time required for the sintering as well as the final porosity of the ceramic.

Figure 2. A) Bovine bone after manual and thermochemical processes to remove organic matter. B) Hydroxyapatite powder resulting from manual milling processes.

The milling processes were performed in an alcohol system. A jar was loaded with 30 vol% of HA, 69.95 vol% of isopropyl alcohol (Lab-Synth), and 0.05 wt% of para-aminobenzoic acid (PABA; Sigma Aldrich). This mixture was placed in a rotatory mill for 48 h, followed by a vibratory mill for 96 h.

Next, 1.2 wt% of polyvinyl butyral (PVB; Butvar B98), previously dissolved in isopropanol, was added and homogenized in a vibratory mill for 2 h.

For the specimens added with nanomaterials, after these 2 h in the vibratory mill, the TiO_2 nanoparticles were weighed at 5% and 8% of the working volume relative to HA, and added to HA with PVB. The mixtures were put back in the vibratory mill for 10 min for homogenization.

The contents of the jars with and without nanoparticles were discharged, and the barbotine was dried with a hot air blower at approximately 80 °C until the liquid was

completely evaporated. Next, the three powders were granulated on sieves (#100 mesh ≤ 150 μm; #150 mesh ≤ 106 μm; #200 mesh ≤ 75 μm).

2.2.1. Conformation and sintering

The experimental ceramics were obtained using the HA powder which did or didn't receive the addition of TiO_2 nanoparticles. Three experimental groups were developed: HA, HA+5%TiO_2, HA+8%TiO_2.

In order to obtain disk-shaped specimens, 0.5 g of the obtained powder was weighed and inserted into a cylindrical container, which generated the conformation of disks with 15 mm diameter and 1.4 mm height, after uniaxial pressing at 100 MPa for 30 seconds.

To complete the compression, the specimens were vacuum encapsulated in elastomeric balloons and pressed by an isostatic press at 200 MPa for 1 min. The specimens were subjected to a sintering furnace (Lindberg/Blue M, Asheville, NC, USA), according to the following temperature gradient: first, from room temperature to 160ºC at a heating rate of 2.7ºC/min; from 160ºC to 600ºC at 4 ºC/ min; from 600ºC to 1100ºC at 5ºC/min; and finally, from 1100ºC to 1300ºC at 6ºC/min. The specimens were maintained at the maximum temperature of 1300ºC for 120 min, followed by the cooling of the furnace up to room temperature.

After sintering, the specimens reached the dimensions of 14 ± 2 mm diameter and 1.2 ± 0.2 mm height. The final dimensions were in accordance with ISO 6872:2015. The study design is shown in Figure 3.

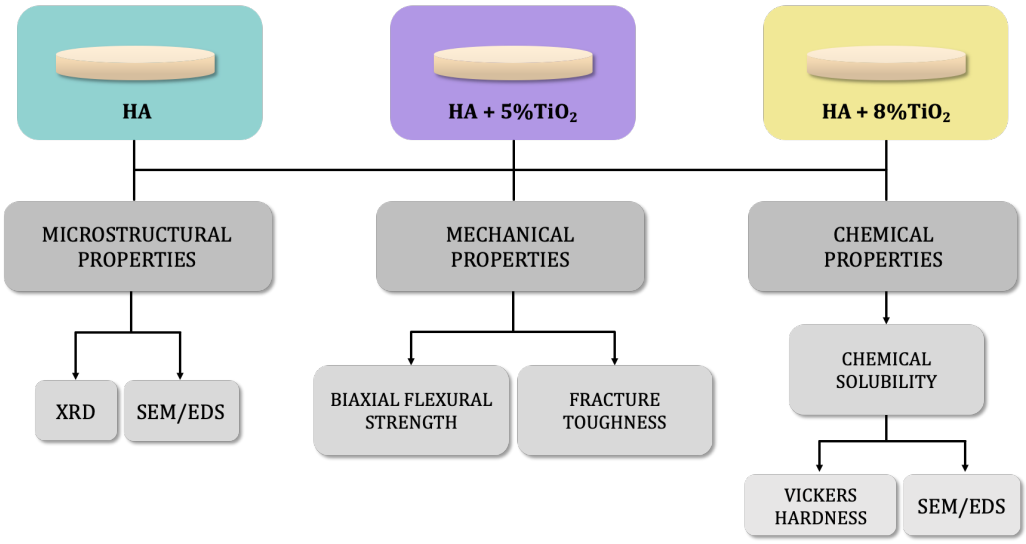

Figure 3. Study design.

2.3. Microstructural properties

2.3.1. X-ray diffraction (XRD)

The initial powders and the three sintered samples were analyzed by an X-ray diffractometer (XRD 7000, Shimadzu, Kyoto, Japan). The scanning was performed on the Bragg-Brentano geometry θ-2θ, using Cu (Kα) radiation, λ = 1.5406 Å, operating at a voltage of 40 kV and a current emission of 30 mA. The data were obtained over 2θ range of 10°− 80° at a scan rate of 2^{o} min^{-1}°.

The software X'pert HighScore Plus (Malvern Panalytical, Malvern, United Kingdom) was used to identify the crystalline phases present in each sample. The crystalline phases were identified by comparing the spectra obtained by the standard cards of the ICSD (Inorganic Crystal Structure Database) database. Furthermore, the program also performed the Rietveld refinements, quantifying the phases present in each sample as well as estimating the crystallite's size.

2.3.2. Scanning electron microscopy (SEM) / Energy Dispersive Spectroscopy (EDS)

A scanning electron microscope (JSM-5600LV, JEOL, Tokyo, Japan) was used to analyze the sintered specimens' microstructure. Before the test, the specimens were put in stubs and a thin layer of conductive carbon was applied on the surface of the specimens using a sputter-coating unit (Denton Vacuum, Moorestown, NJ, USA). External and fractured surfaces were observed at 500x, 1000x, 2000x and 5000x magnifications.

The elemental compositions of each specimen were determined by EDS analysis. The specimens were subjected to SEM imaging at 35x magnification. Three sites of interest from each specimen were scanned for further comparison.

2.4. Mechanical properties

2.4.1. Fracture toughness (K_{IC})

Two specimens from each group were added in PVC cylinders and epoxy resin was poured into them (Piraglass Ltda., Piracicaba, SP, Brazil). After resin polymerization, the surface of each specimen was finished by silicon carbide papers (#150, #240,

#320, #400, #600, #800 e #1200) and polished with felt discs and diamond abrasive paste of 4 µm, 2 µm and 1 µm in a semiautomatic sander (APL-4, Arotec, São Paulo, SP, Brazil), followed by 10 min of sonication with distilled water to clean and remove any polishing residue (Maxi Clean 750, UNIQUE UltraSonic, Indaiatuba, SP, Brazil).

The indentation fracture (IF) method was used to estimate the fracture toughness. A microhardness tester VMHT Mot (Leica, Wetzlar, Germany) with a Vickers indenter was used for the test. Five indentations were performed on each specimen. For each indentation, the microhardness tester was programmed to generate a load of 500 gf for 15 seconds, which was sufficient to generate radial cracks from the indentation vertices. The length of produced crack (*c*) and half of indentation diagonal (*a*) were measured to calculate the *c/a* ratio (Figure 4). When *c/a* < 2.5, it is suggested that the crack is Palmqvist type, and when *c/a* > 2.5, radial-median type [22]. Fracture toughness values were then calculated using the correct equation for the corresponding crack type.

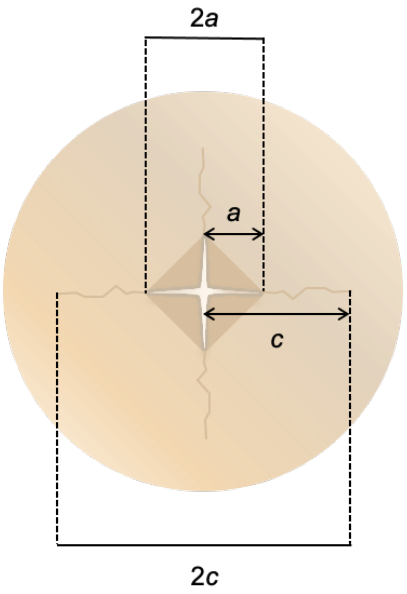

Figure 4. Values measured to obtain the type of crack produced with indentation. "*a*" corresponds to half of indentation diagonal and "*c*", to length of crack produced measured from the center of the indentation.

2.4.2. Biaxial flexural strength (BFS)

Thirty specimens from each group were subjected to the biaxial flexural strength test using a universal testing machine (K2000 MP, Kratos, Cotía, Brazil) and a specific device (OD36, Odeme Dental Research, Luzerna, Brazil), according to ISO 6872:2015 guidelines (Figure 5A). In the device, each disk was placed on three steel balls with a

diameter of 3.5 mm each and positioned 120º apart on a circular support with a diameter of 10 mm. A load was applied in the center of the specimen by a piston with a diameter of 1.4 mm, at a crosshead speed of 0.5 mm/min until failure (Figure 5B). Fracture load data, in newtons (N), were collected and the following equation was used to calculate the flexural strength (MPa):

$$\sigma = -0{,}2387P(X - Y)/b^2$$

where σ is the maximum tensile stress (MPa), P is the total load which leads to fracture (N), b is the specimen thickness at fracture site (mm), and X and Y are calculated according to:

$$X = (1+\upsilon)\ln(r_2/r_3)^2 + [(1-\upsilon)/2](r_2/r_3)^2$$

$$Y = (1+\upsilon)[1+\ln(r_1/r_3)^2] + (1-\upsilon)(r_1/r_3)^2$$

where υ is Poisson's ratio (0.25), r_1 is the radius of support circle (mm), r_2 is the radius of loaded area (mm) and r_3, the radius of specimen (mm).

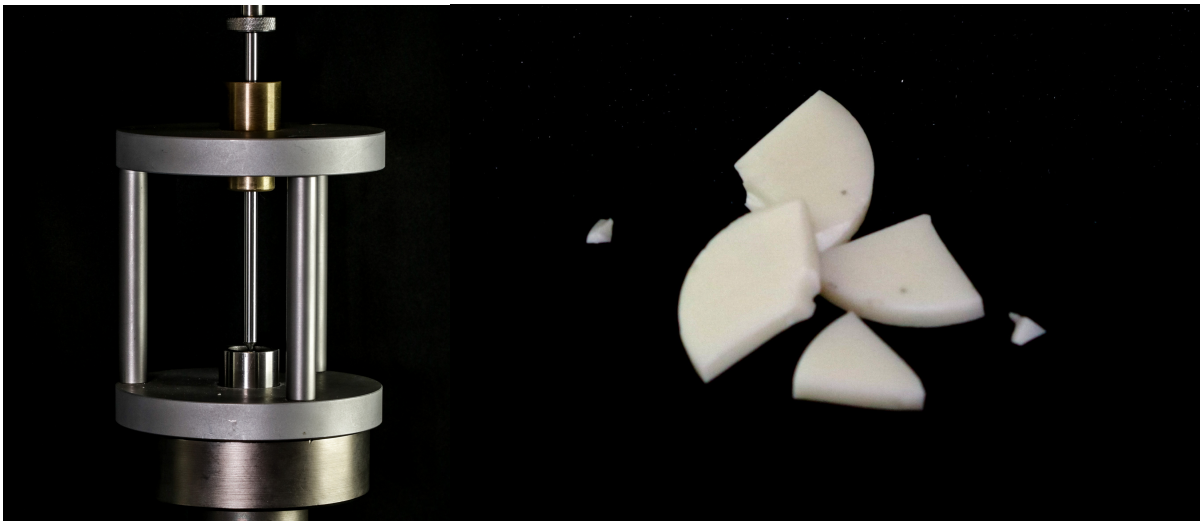

Figure 5. A – Device developed to content the ISO 6872 standard recommendations in the biaxial flexural strength test. B – Specimen fractured after the mechanical test.

2.5. Chemical properties

2.5.1. Chemical solubility

The current standard ISO (6872:2015) does not specify the specimen's number or shape for the chemical solubility test in dental ceramics, it is only required that the surface area exposed to the solution be at least 30 cm^2.

The surface area of each disk was determined by measuring the radius (r) and height (h) of each one (Figure 6) and applying these values to the formula for total surface area of a cylinder ($2.\pi.r^2 + 2.\pi.r.h$), where $\pi = 3.14$. With the surface area of each disk calculated, eleven disks from each group were used for this test, in a manner that the number of specimens in each group had a total surface area above 30 cm^2 (Table 1).

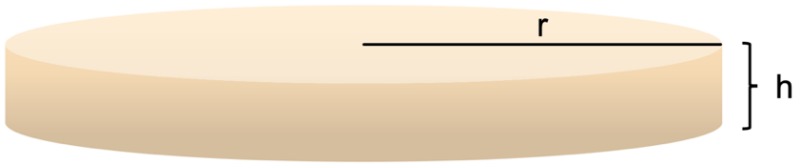

Figure 6. Measured dimensions on each disk specimen to be applied in the formula for the area of a cylinder.

All specimens' surfaces were finished and polished by silicon carbide papers #600, #800, #1200, #1500, #2000 and #2500 as well as utilizing felt discs and aluminum oxide paste.

Following the ISO recommendations, the disks were ultrasonically cleaned (USC-1800, UNIQUE, Indaiatuba, SP, Brazil) in deionized water for 15 min, dried for 4 hours at 150 ± 5 ºC in a thermostatically controlled oven (Thoth Equipment's, Piracicaba, SP, Brazil) and weighed on an analytical scale with 0.1 mg precision (AR2140, Ohaus Adventurer, Barueri, SP, Brazil). Next, specimens were immersed in 100 mL of 4% acetic acid (by volume) in a 250 mL Pyrex® glass bottle. The glass bottle was closed and placed in a preheated dry heat oven to 80 ± 2 °C for 16 hours. After which, the specimens were once again ultrasonically washed with deionized water for 15 min, dried for 4 hours at 150 ± 5 °C and reweighed. Chemical solubility was determined by calculating the mass loss in $\mu g/cm^2$, using the following equation:

$$\text{Chemical solubility } (\mu g/cm^2) = \text{weight loss } (\mu g) / \text{surface area } (cm^2)$$

Considering changes could happen at the surface during chemical solubility testing, characterization tests such as SEM, EDS and Vickers hardness were carried out to investigate the effects of exposure to 4% acetic acid on specimens from the three groups (HA, HA+5%TiO_2 e HA+8%TiO_2).

2.5.1.1. Vickers hardness (VH)

Vickers hardness was measured, before and after the chemical solubility test, using a microhardness tester with a Vickers indenter (Wilson Tukon 1202, Buehler, Illinois, USA) with a 300 gf load and a dwell time of 15 seconds for the 11 specimens from each group. Using the Buehler Omnimet MHT software, five indentations were measured per specimen, and an average hardness was calculated.

Groups	Specimens (n=11)	Radius (cm)	Height (cm)	Individual surface area (cm^2)	Total surface area (cm^2)
HA	1	0.65	0.12	3.14	32.18
	2	0.61	0.12	2.86	
	3	0.62	0.12	2.86	
	4	0.59	0.13	2.68	
	5	0.61	0.12	2.83	
	6	0.65	0.12	3.12	
	7	0.65	0.12	3.13	
	8	0.61	0.13	2.84	
	9	0.65	0.12	3.15	
	10	0.62	0.12	2.86	
	11	0.60	0.13	2.71	
HA + 5%TiO_2	1	0.64	0.12	3.08	31.74
	2	0.65	0.12	3.10	
	3	0.61	0.12	2.77	
	4	0.60	0.12	2.74	
	5	0.61	0.12	2.77	
	6	0.60	0.12	2.74	
	7	0.61	0.12	2.76	
	8	0.65	0.13	3.14	
	9	0.65	0.12	3.11	
	10	0.60	0.12	2.75	
	11	0.61	0.12	2.76	
HA + 8%TiO_2	1	0.64	0.12	3.03	31.06
	2	0.64	0.12	3.05	
	3	0.60	0.12	2.75	
	4	0.61	0.12	2.79	
	5	0.60	0.13	2.78	
	6	0.61	0.12	2.79	
	7	0.61	0.12	2.82	
	8	0.60	0.12	2.75	
	9	0.60	0.12	2.74	
	10	0.61	0.12	2.78	
	11	0.61	0.12	2.77	

Table 1. Surface area of each specimen and number of specimens required to have at least 30cm^2 of surface area.

2.6. Statistical analysis

Data obtained from fracture toughness, chemical solubility and Vickers hardness were tabulated and subjected to normality (Shapiro-Wilk) and homoscedasticity (Levene) tests. In case of parametric distribution, data were statistically evaluated using one-way analysis of variance (ANOVA), for independent groups, and through two criteria repeated-measures ANOVA, for paired groups, followed by post-hoc comparisons test by Tukey, with significance level set at $p < 0.05$. In case of non-parametric distribution, the Kruskal-Wallis test was used. Data sets were analyzed using statistical software Jamovi (Jamovi version 2.0, Sydney, Australia).

Biaxial flexural strength data were analyzed by the Weibull 2-parameter statistical analysis (Weibull++, Reliasoft, Tucson, AZ, USA). The probability of failure *versus* stress and the Weibull modulus (m) *versus* characteristic stress (σ0) (reliability) were performed with 90% confidence levels.

3. RESULTS

3.1. XRD

With regards to the initial powders (before sintering), the XRD pattern of TiO_2 shows that only the anatase phase (9852-ICSD) was found. Typical crystalline content of HA (26204-ICSD) was found for initial powder from bovine bone. While for the samples sintered at 1300ºC, in the HA group (without nanoparticles) a non-characteristic peak was found and corresponds to ß-TCP (6191-ICSD), another ceramic from calcium phosphate family. For the sintered samples containing 5% and 8% of TiO_2 nanoparticles, the presence of HA and TiO_2 was not identified. The identified peaks were ß-TCP and also a perovskite, calcium titanate ($CaTiO_3$) (74212-ICSD) (Figure 7). The weight fraction (%) of each phase based on relative peak intensity was estimated by Rietveld refinement and can be seen in Table 2.

Using Scherrer's equation, $L=(0.94*\lambda)/(\beta*\cos\theta)$, where L is the crystallite's size (∅), λ is wavelength of the source used in XRD equipment, β is width at peak's half height and θ is the peak angle, we were able to estimate that the crystallites were nanoparticles (HA crystallite = 40nm; TiO_2 crystallite = 50nm).

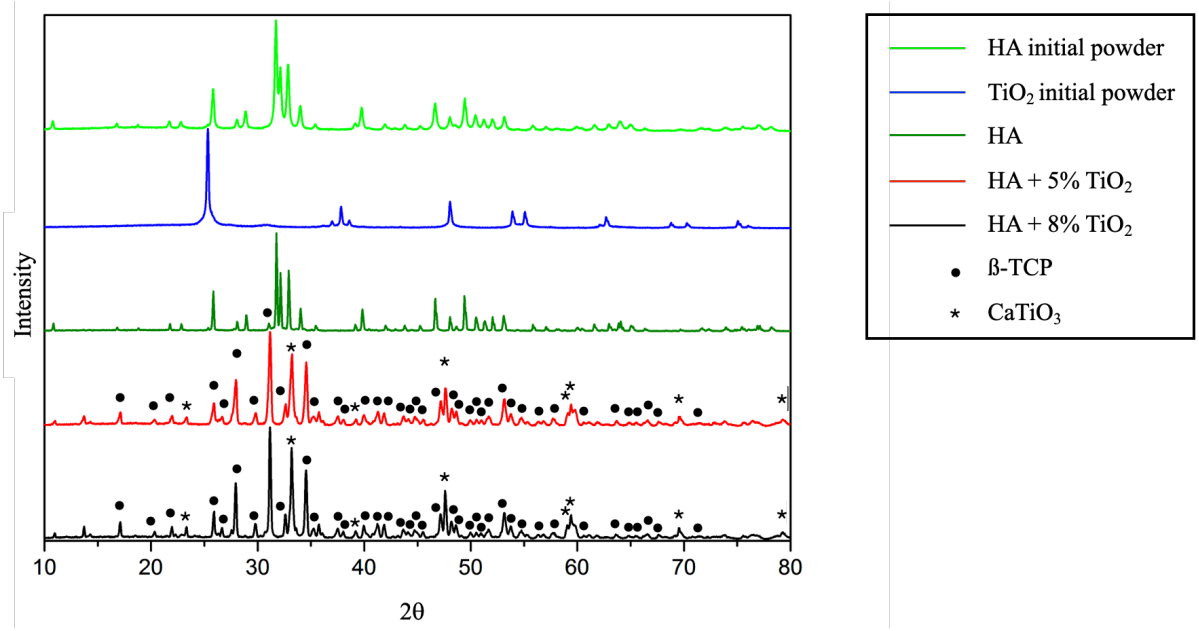

Figure 7. DRX patterns of initial powders and experimental ceramics.

	HA (26204-ICSD)	ß-TCP (6191-ICSD)	$CaTiO_3$ (74212-ICSD)
HA	91,7%	8,3%	-
HA + 5%TiO_2	-	77,7%	22,3%
HA + 8%TiO_2	-	75,9%	24,1%

Table 2. Phase compositions obtained by Rietveld analysis.

3.2. SEM/EDS

SEM micrographs showing the three sintered groups' external surfaces microstructure are presented in Figure 8 and fractured surfaces are presented in Figure 9. The surface of sintered samples showed a dense fully crystalline matrix, with a good densification degree. Another phase's uniform distribution is also observed on the dense matrix, both for the TiO_2 additions of 5% as well as the 8% one. Observing the bulk of sintered samples, a different pattern of the surface can be seen, where the presence of porosities can be observed. The bulk of the three materials is very similar with regards to their microstructure, with presence and number of pores apparently similar.

The EDS results are shown in section 3.5. (Chemical solubility, VH and EDS analysis).

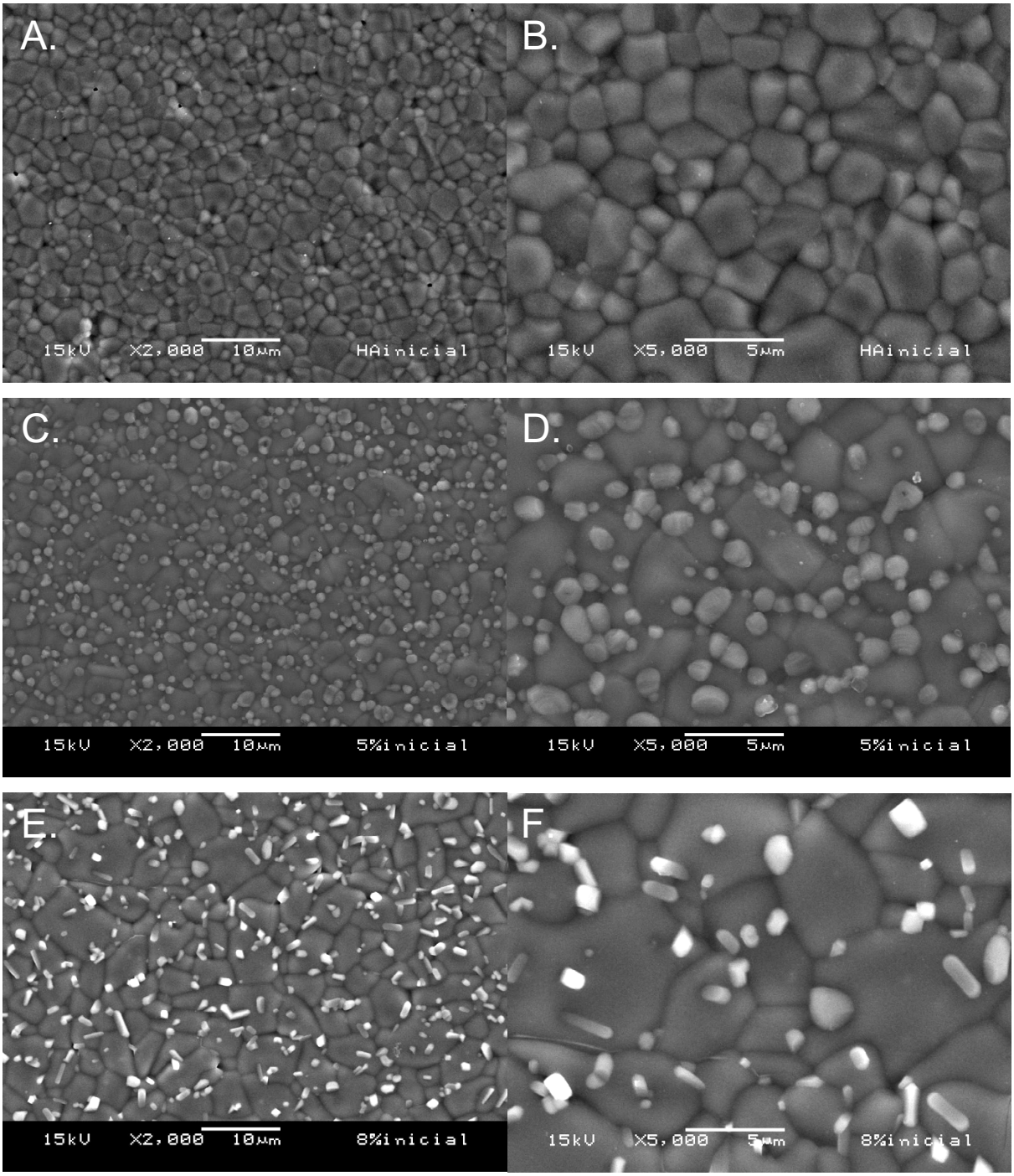

Figure 8. Micrographs of the external surface of sintered specimens. (A, B) HA. (C, D) HA+5%TiO_2. (E, F) HA+8%TiO_2.

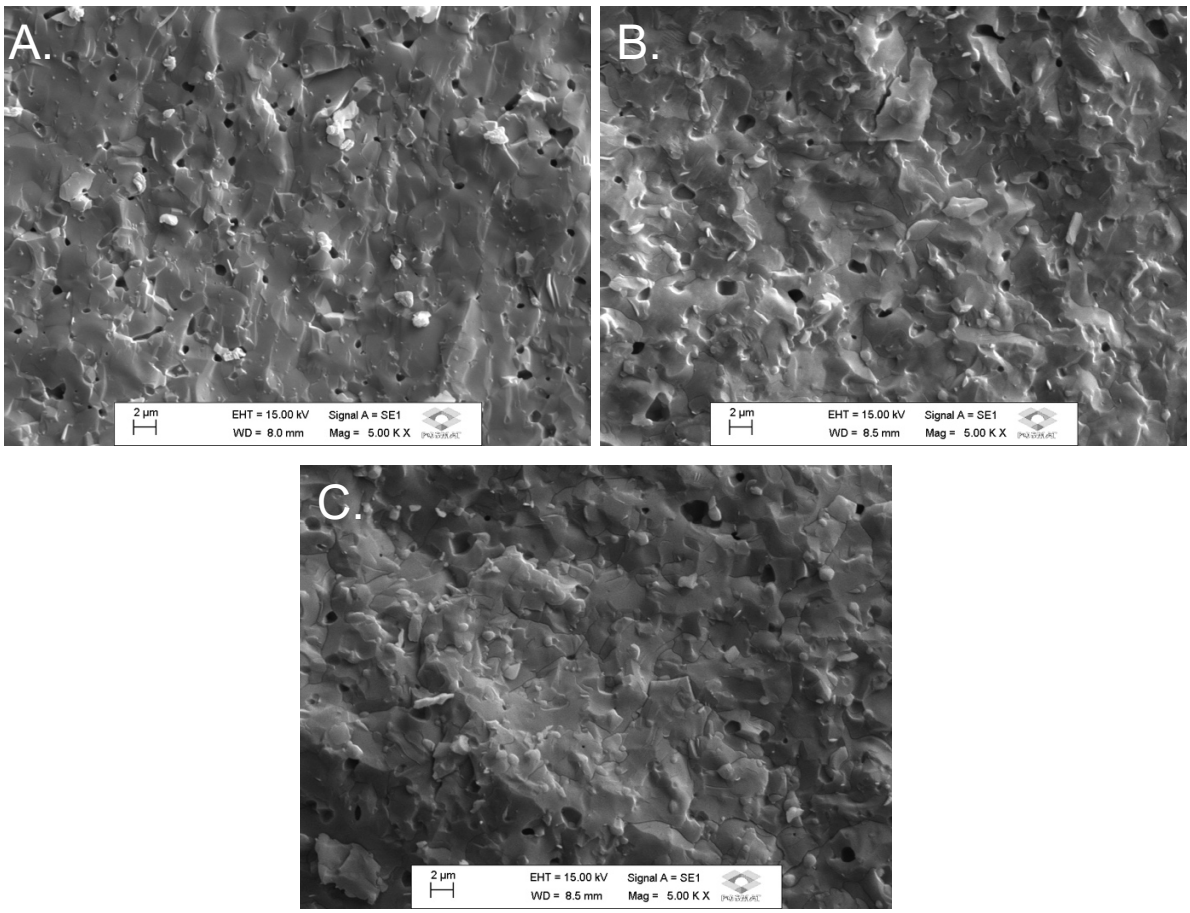

Figure 9. Micrographs of the fractured surface (bulk) of sintered specimens. (A) HA; (B) HA+5%TiO_2; (C) HA+8%TiO_2.

3.3. Fracture toughness (K_{IC})

The formula's choice for calculating fracture toughness by the IF method depends on the type of crack that is formed. In this study, the Anstis equation was used, as the *c/a* ratio indicated that the cracks were of the radial-median type. Fracture toughness was calculated by the following equation:

$$K_{1C} = A\left(\frac{E}{H}\right)^{1/2}\frac{P}{c^{3/2}},$$

where *A* is a constant determined by Anstis et al. (1981) with a value of 0.016, *E* is the Young's modulus (GPa), *H* is the Vickers hardness (GPa) obtained at the indentation moment, *P* is the applied load (N) and *c* is the crack length produced (µm), measured from the center of the indentation.

Fracture toughness data were normally distributed and analyzed using parametric test ANOVA. A significant difference was found among the groups ($p < 0.05$). IF toughness was higher for HA+5%TiO_2 (1.34 ± 0.26 MPa.$m^{1/2}$) and HA+8%TiO_2 (1.28 ± 0.21 MPa.$m^{1/2}$) than for HA (0.65 ± 0.10 MPa.$m^{1/2}$). However, among the groups containing 5% and 8% of the TiO_2 nanoparticles, no significant difference was found ($p > 0.05$).

The cracks' profile produced by the three groups are shown on the micrographs of Figure 10. It is possible to observe a decrease in crack length in the groups containing TiO_2 nanoparticles.

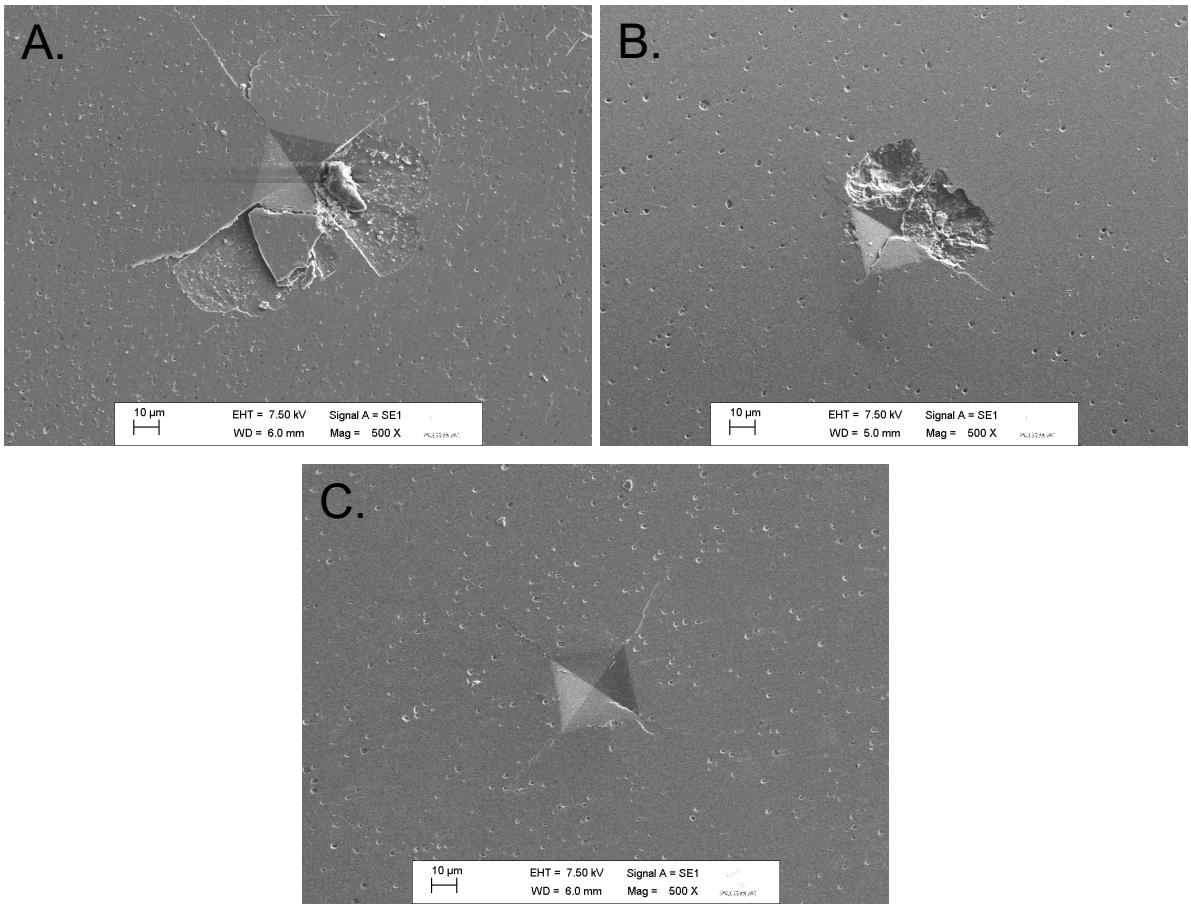

Figure 10. Micrographs obtained after the IF method. (A) HA; (B) HA+5%TiO_2; (C) HA+8%TiO_2. Note a decrease in crack length in groups with TiO_2 nanoparticles.

3.4. BFS and Weibull analysis

The use level probability Weibull curves and contour plot of the three groups after biaxial flexural strength tests are shown in Figures 11 and 12, respectively. Table 3 shows the results of Weibull statistical analysis. The Weibull modulus (*m*) - an indicator

of reliability - and characteristic stress (MPa) - which indicates the stress in which 63.2% of the specimens of each group may fail - are represented in the contour plot. Significant differences were identified considering the non-overlap of the contours. HA demonstrated the highest characteristic stress values, which is statistically different from HA+5%TiO_2 and HA+8%TiO_2. However, regarding the analysis of the Weibull modulus (*m*), the overlap between contours when projected on the Y axis of the graph, indicates the absence of significant differences for the three groups and indicates they are homogeneous.

	Characteristic Stress (σ0)	Weibull Modulus (*m*)
HA	295.8 (273-319)[a]	5.3 (3.9-7.0)[a]
HA + 5%TiO_2	235.1 (223-247) [b]	8.0 (5.9-10.4)[a]
HA + 8%TiO_2	214.4 (200-228)[b]	6.2 (4.6-8.0)[a]

Table 3. Results of Weibull statistical analysis. Characteristic stress (MPa) and Weibull modulus (*m*) with their respective minimum and maximum. Different letters indicate significant difference between materials ($p < 0.05$).

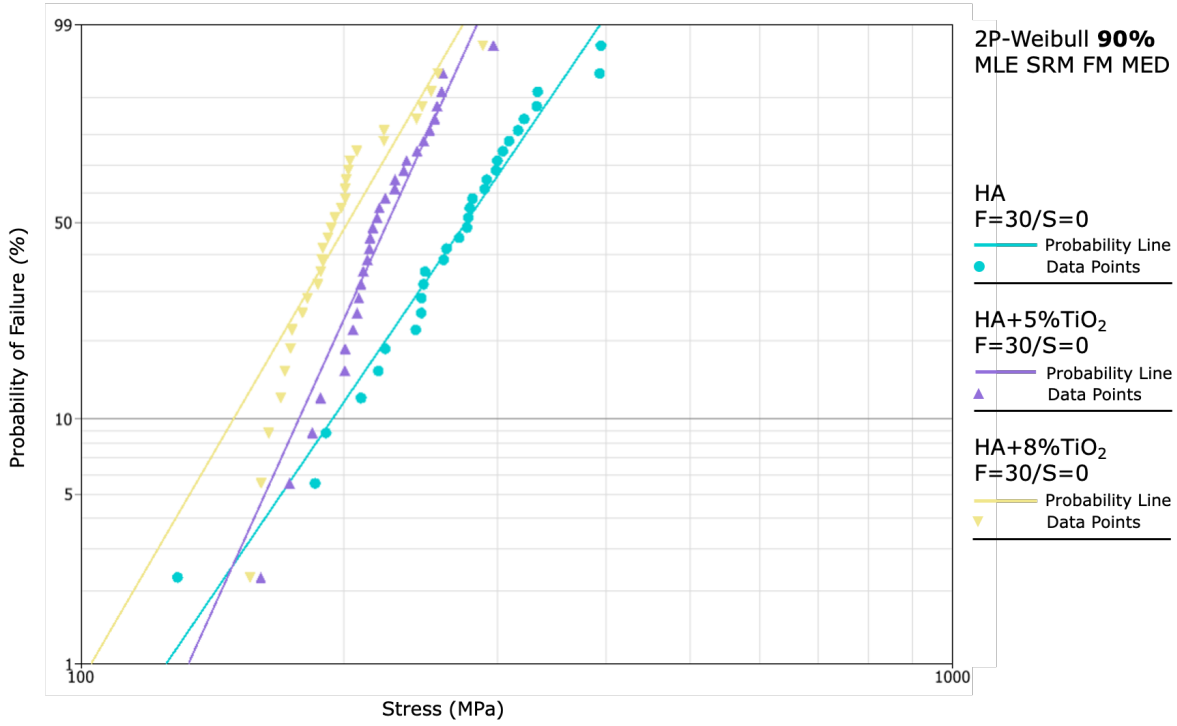

Figure 11. Use level probability Weibull, showing the probability of failure as a function of stress (MPa) of the three experimental groups after biaxial flexural strength tests.

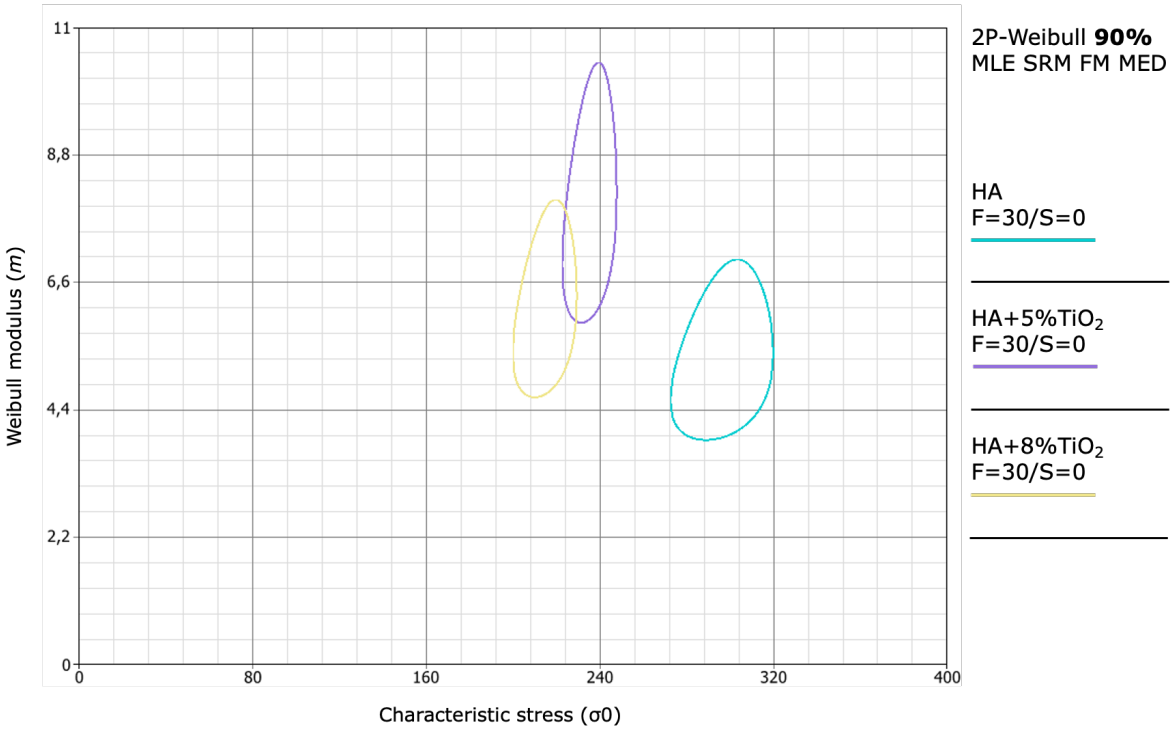

Figure 12. Contour Plot showing Weibull modulus (*m*) as a function of Characteristic stress (MPa). The non-overlap between contours indicates statistically significant difference.

3.5. Chemical solubility, VH and EDS analysis

Chemical solubility data indicated a violation of normality and therefore, were analyzed nonparametrically by Kruskal-Wallis. No significant difference was found among the groups HA (6536, 6277;7877 μg/cm^2), HA+5%TiO_2 (6654, 6099;8551 μg/cm^2) and HA+8%TiO_2 (8548, 8481;8654 μg/cm^2) ($p > 0.05$). The box-plot of solubility results can be seen in Fig. 13. These results placed all tested experimental ceramics above the 2000 ug/cm^2 limit set by the ISO standard (6872:2015) for a dental ceramic material (see Table 4).

Fig. 14(A-I) show SEM micrographs of the surfaces after the chemical solubility test. For all the tested materials, the micrographs showed great damage and high surface roughness after the solubility test. Moreover, micrographs also show the lack of some particles from the surface after the test. In Fig. 14D and 14G it is possible to observe, at 200x magnification, elevations formations on the surface of specimens with the nanoparticles, which didn't happen in the HA specimens (Fig. 12A).

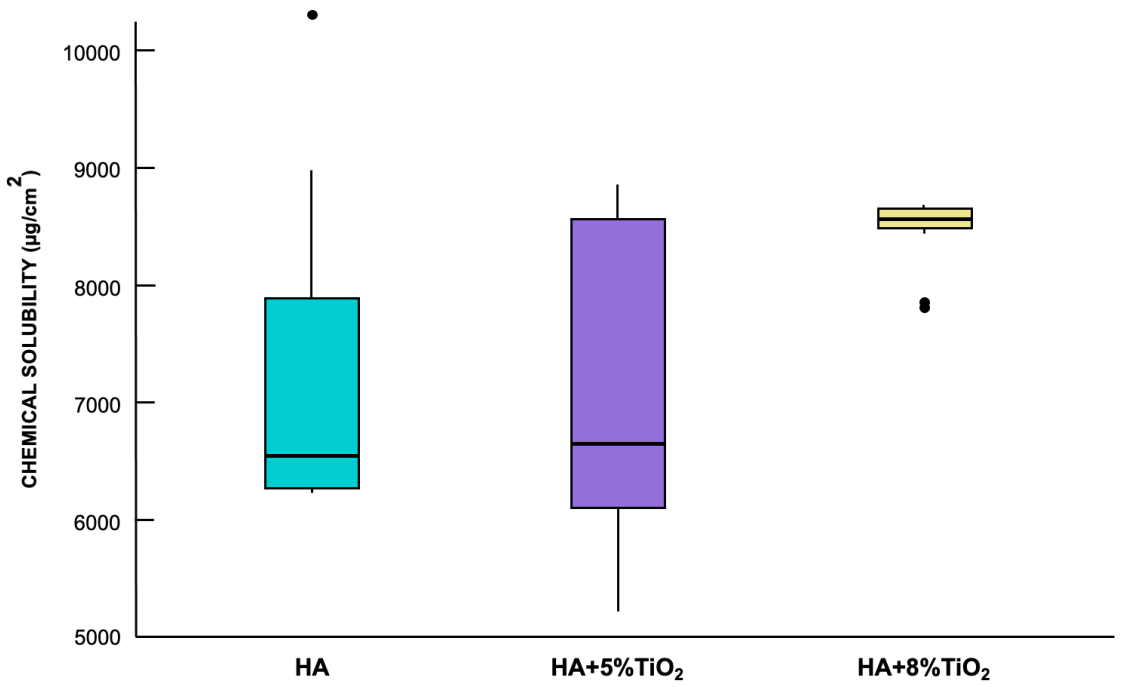

Figure 13. Box-plot. The Kruskal-Wallis test found no significant difference between the chemical solubility values of the experimental groups.

Class	Recommended Clinical Indications	Mechanical and chemical properties		
		Flexural strength (MPa)	Fracture toughness (MPa.√m)	Chemical solubility (µg/cm²)
1	a) Monolithic ceramic for single-unit anterior prostheses, veneers, inlays, or onlays adhesively cemented. b) Ceramic for coverage of a metal framework or a ceramic substructure.	50	0.7	<100
2	a) Monolithic ceramic for single-unit anterior or posterior prostheses adhesively cemented.	100	1	<100
	b) Partially or fully covered substructure ceramic for single-unit anterior or posterior prostheses adhesively cemented.	100	1	<2000
3	a) Monolithic ceramic for single-unit anterior or posterior prostheses and for three-unit prostheses not involving molar restoration adhesively or non-adhesively cemented.	300	2	<100
	b) Partially or fully covered substructure for single-unit anterior or posterior not involving molar restoration adhesively or non-adhesively cemented.	300	2	<2000
4	a) Monolithic ceramic for three-unit prostheses involving molar restoration.	500	3.5	<100
	b) Partially or fully covered substructure for three-unit prostheses involving molar restoration.	500	3.5	<2000
5	Monolithic ceramic for prostheses involving partially or fully covered substructure for four or more units or fully covered substructure for prostheses involving four or more units.	800	5	<100

Table 4. Classification of ceramics for fixed prostheses by clinical use with the mechanical and chemical properties recommended by ISO 6872:2015 and the findings for experimental ceramics.

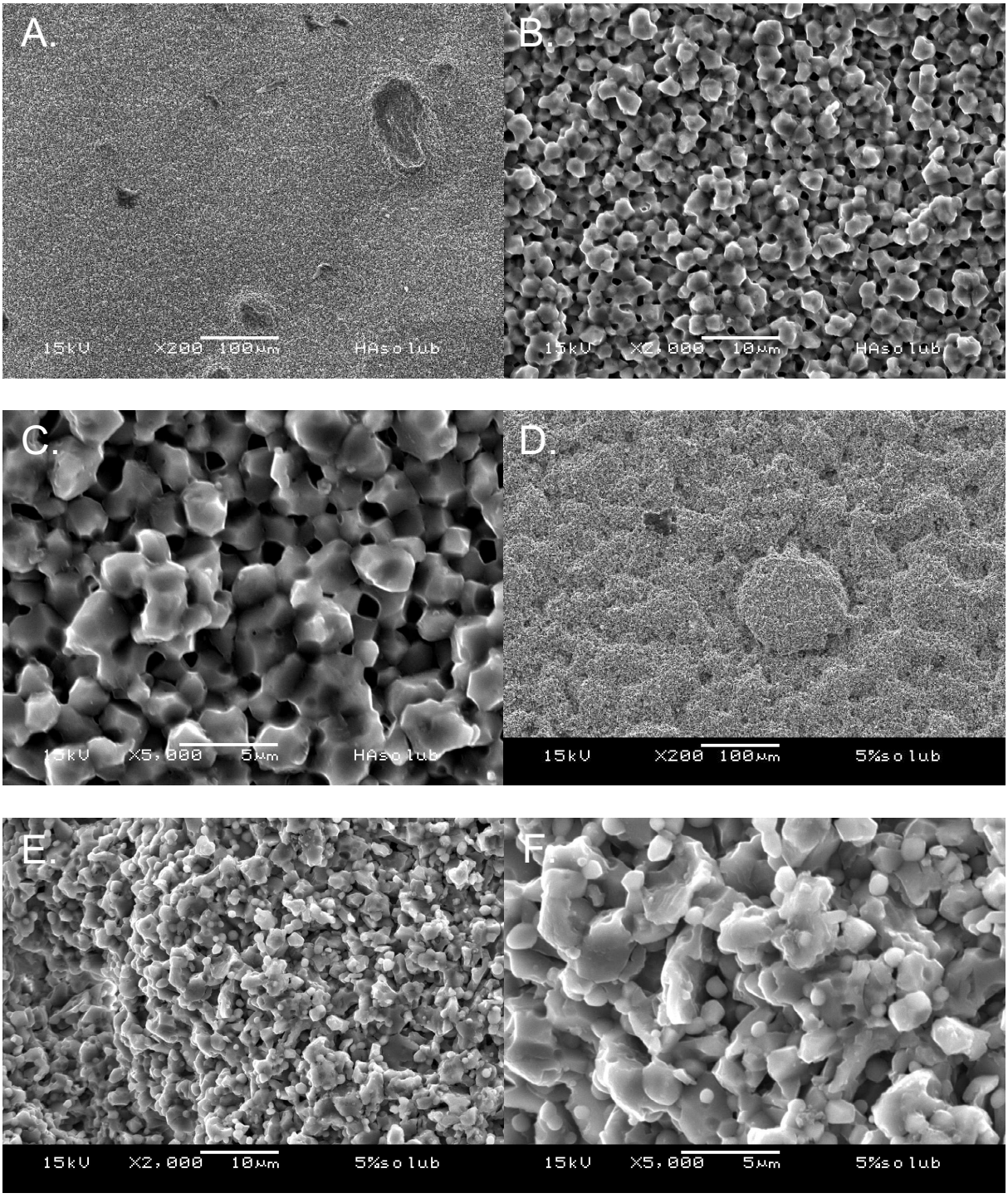
A.
15kV X200 100µm HAsolub
B.
15kV X2,000 10µm HAsolub
C.
15kV X5,000 5µm HAsolub
D.
15kV X200 100µm 5%solub
E.
15kV X2,000 10µm 5%solub
F.
15kV X5,000 5µm 5%solub

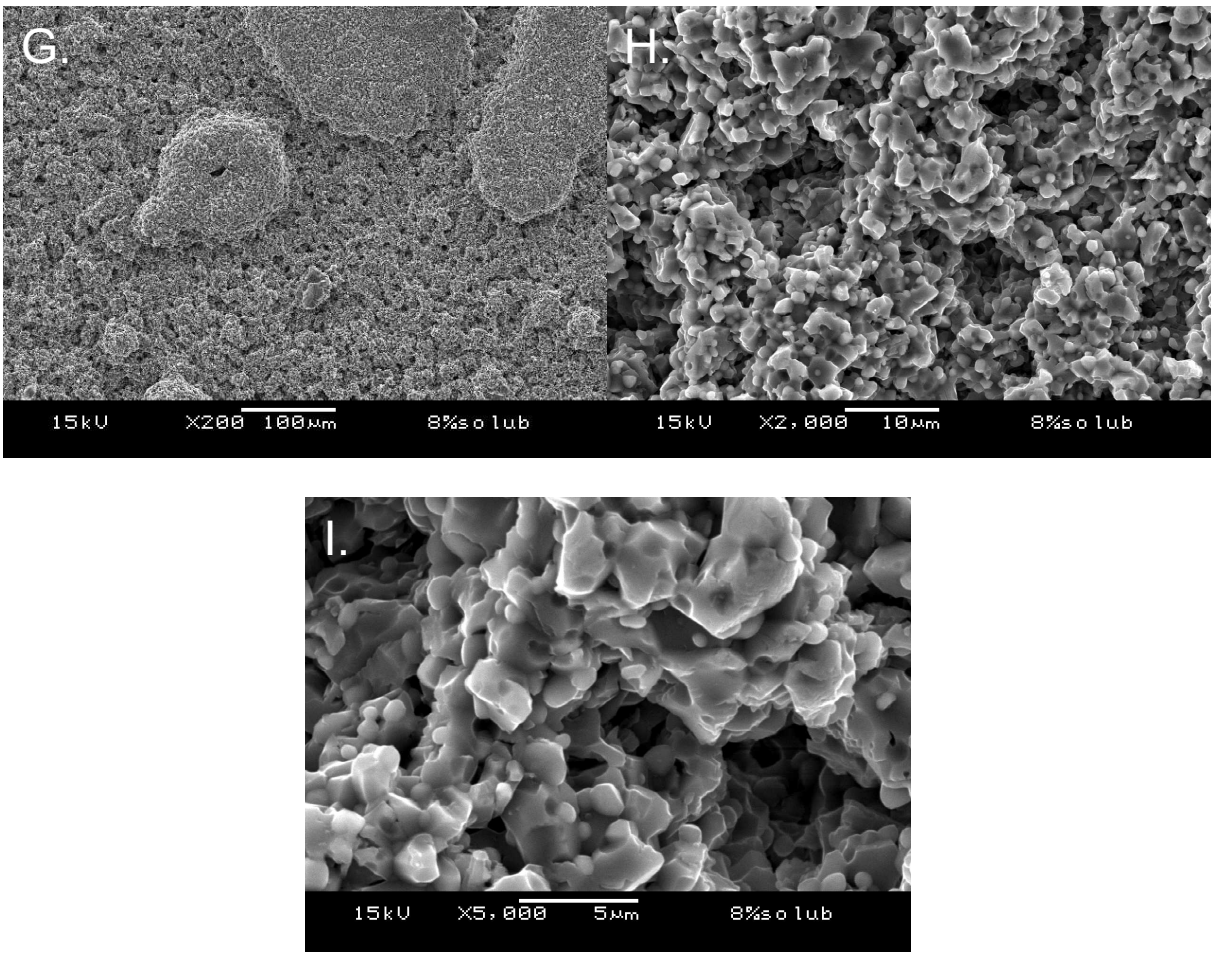

Figure 14. Surface of the experimental ceramic groups in 200x, 2000x and 5000x after the chemical solubility test. A, B, C - HA group. D, E, F - HA+5%TiO_2 group. G, H, I - HA+8%TiO_2.

Specimens' EDS scans were obtained of pre- and post-solubility testing. Three randomly selected spectra were representatives of each specimen. The EDS analysis showed that the surface of HA was mainly composed of calcium (Ca) and phosphorus (P). The quantitative findings are summarized in Table 5. For HA+5%TiO_2 and HA+8%TiO_2 the EDS analysis showed that the HA group's surface was mainly composed of Ca, P and titanium (Ti), the quantitative findings are summarized in Table 6 and 7, respectively. There was a significant decrease in phosphorus in the composition after the solubility test for all groups ($p<0.05$). A significant decrease in Ti can also be observed in the HA+8%TiO_2 group ($p<0.05$).

Element	wt% Pre-solubility				wt% Post-solubility			
	S1	S2	S3	Mean ± SD	S1	S2	S3	Mean ± SD
Ca	72.5	72.1	72.4	72.3 ± 0.2	73.6	73.3	73.4	73.4 ± 0.2
P	27.5	27.9	27.6	27.7 ± 0.2*	26.4	26.7	26.6	26.6 ± 0.2*
Ti	-	-	-	-	-	-	-	-

Table 5: The table shows the detected elements in HA specimens as determined by EDS. S1, S2 and S3 indicate the spectra. The presence of asterisk indicates a significant difference within the same group.

Element	wt% Pre-solubility				wt% Post-solubility			
	S1	S2	S3	Mean ± SD	S1	S2	S3	Mean ± SD
Ca	63.5	63.5	64.0	63.7 ± 0.3	63.5	64.2	63.5	63.7 ± 0.4
P	24.9	25.0	24.9	25.0 ± 0.04*	20.3	21.3	20.7	20.8 ± 0.5*
Ti	11.6	11.5	11.1	11.4 ± 0.3	16.2	14.5	15.8	15.5 ± 0.9

Table 6: The table shows the detected elements in HA+5%TiO_2 specimens as determined by EDS. S1, S2 and S3 indicate the spectra. The presence of asterisk indicates a significant difference within the same group.

Element	wt% Pre-solubility				wt% Post-solubility			
	S1	S2	S3	Mean ± SD	S1	S2	S3	Mean ± SD
Ca	57.2	58.1	56.3	57.2 ± 0.9	64.3	64.0	64.8	64.4 ± 0.4
P	25.3	25.8	24.8	25.3 ± 0.5*	20.5	21.4	21.3	21.1 ± 0.5*
Ti	17.5	16.2	19.0	17.5 ± 1.4*	15.2	14.6	14.0	14.6 ± 0.6*

Table 7: The table shows the detected elements in HA+8%TiO_2 specimens as determined by EDS. S1, S2 and S3 indicate the spectra. The presence of asterisk indicates a significant difference within the same group.

As for the Vickers hardness data before and after the solubility test, repeated-measures analysis of variance (ANOVA) showed that the average hardness of the samples significantly decreased after the chemical solubility test ($p < 0.05$) for the same group. When comparing the three groups initial and final hardness values, no significant differences were found between them (Figure 15). The results showed that the hardness of HA was reduced by 14.5% after the chemical solubility test, by 26.7% for the group with 5% nanoparticles and approximately 31% for the group with 8% (Figure 16). The mean and standard deviation values of VH pre- and post-solubility are in Table 8.

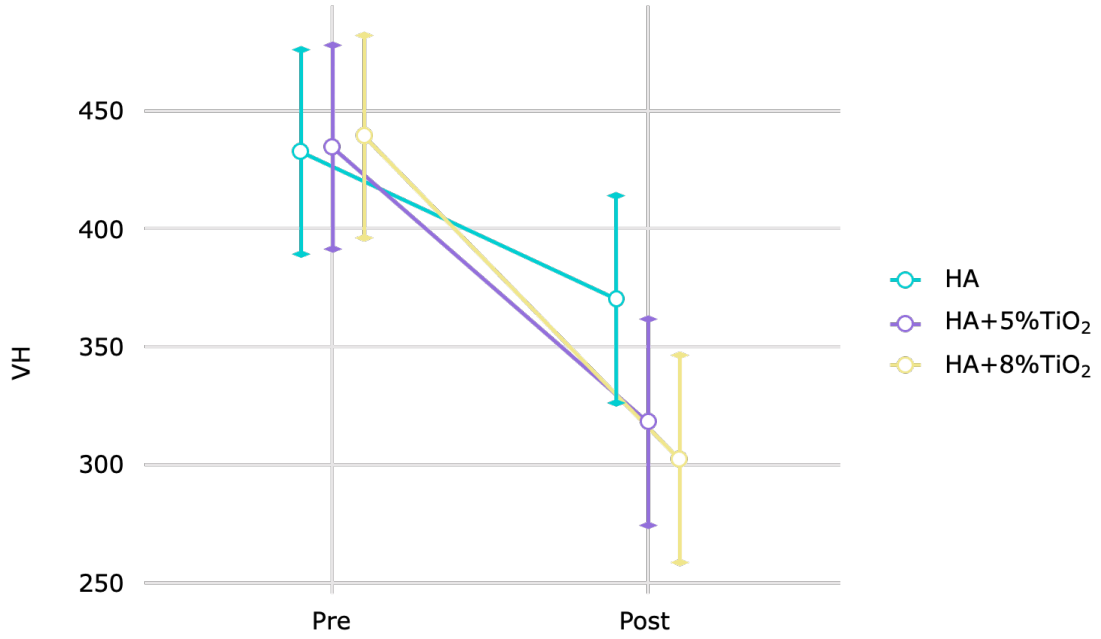

Figure 15. The graph presented above shows that there were significant differences when the same group was compared pre- and post-solubility test. However, between the three groups there is no significant difference in Vickers hardness before or after the solubility test.

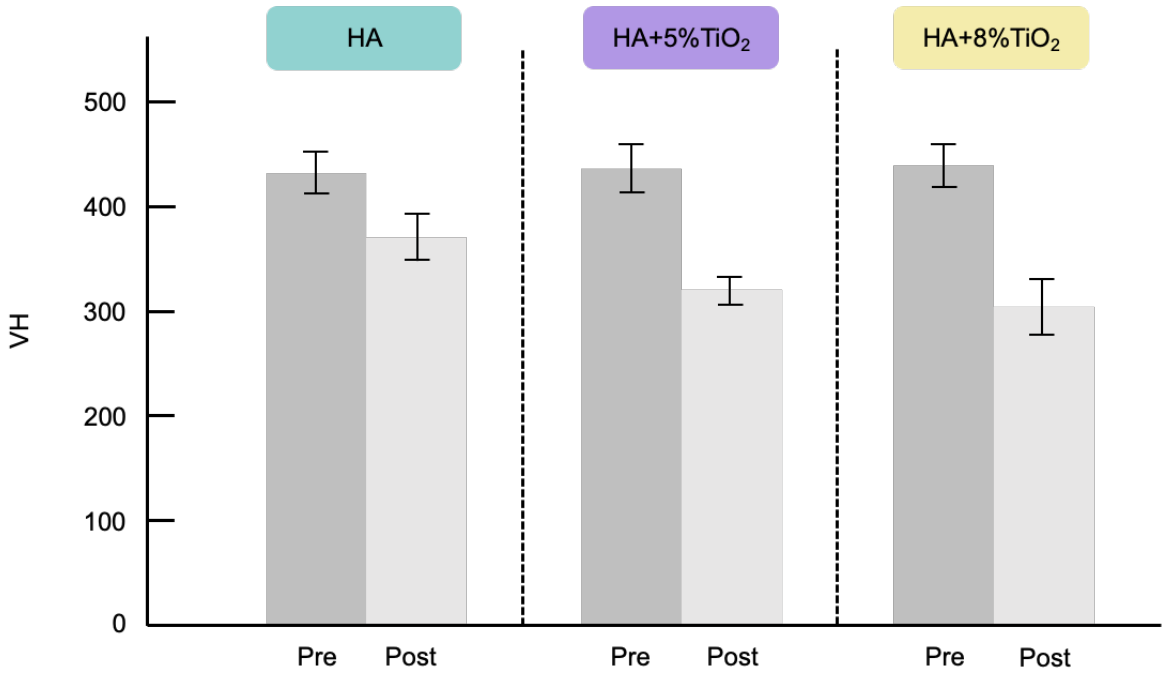

Figure 16. Difference in the Vickers hardness mean values in the three groups pre- and post-solubility test (n=11).

	Vickers hardness pre-solubility (VH)	Vickers hardness post-solubility (VH)
HA	433 ± 67 [a]	370 ± 75 [b]
HA + 5%TiO_2	434 ± 76 [a]	318 ± 43 [b]
HA + 8%TiO_2	439 ± 66 [a]	303 ± 88 [b]

Table 8. The mean and standard deviation values of VH pre- and post-solubility. Groups having different superscript letter were significantly different ($p < 0,05$).

4. DISCUSSION

This study proposed the development and characterization of a new ceramic for dental use made from HA, extracted from bovine bones, as an idea of reusing these solid wastes to turn them into a sustainable and low-cost material. Besides, the addition of TiO_2 nanoparticles to this material was carried out in an attempt to improve its mechanical and chemical properties.

According to our findings, the XRD pattern of the TiO_2 initial powder shows that only the anatase phase was found. This result was already expected by the temperature (450 ºC) and time (2h) used in the sol-gel route [23, 24]. The XRD pattern showed that only pure HA was found in the bovine HA initial powder. This indicates that the powder obtained from bovine bone consists of pure HA and, at the calcination temperature of 900 ºC, HA did not decompose into other crystalline phases. However, increasing the temperature, for HA samples sintered at 1300 ºC, it was possible to observe in diffractogram the appearance of a peak not found at 900 ºC, corresponding to ß-TCP, indicating that at 1300 ºC there was partial decomposition of HA. In the sintered samples containing the TiO_2 nanoparticles, the Rietveld refinement indicated that the entire composition of HA and TiO_2 was converted into ß-TCP and $CaTiO_3$.

Kusrini & Sontang (2012) [25] demonstrated by DTA analysis that the formation of a new phase of bovine bone powder took place between 1125 and 1227 ºC. The authors recommended that the ideal temperature for sintering is around 1000 ºC for 3h. The study by Rincón-López et al. (2018) [26] did not observe the decomposition of bovine HA at the sintering temperature of 1200 °C. Although hydroxyapatite is known for its thermal instability [4, 27], studies reported that at sintering temperatures greater or equal to 1300 ºC, HA decomposition was not observed [28, 29], which differs from what was found in this study. However, these studies researched synthetic HA.

Apparently, synthetic HA and bovine HA have different behaviors. In addition, other factors than sintering temperature may be related to these findings, such as the synthesis method, sintering time, heating or cooling rate time, and even the stoichiometry of the obtained material [2, 4, 8, 30, 31].

ISO 6872 specifies guidelines and appropriate testing methods for assessing dental ceramic materials, including methods to evaluate the flexural strength, fracture toughness and chemical solubility of dental ceramics. According to the values obtained in the tests, ceramic materials can be classified and recommended for specific clinical use (Table 8). Based on these recommendations, it was possible to mechanically and chemically characterize the new experimental calcium phosphate ceramic.

According to the data obtained in the fracture toughness test, the material without nanoparticles (HA group) did not reach the minimum value to be used as a dental ceramic (< 0.7 MPa√m). However, the addition of 5% and 8% of nanoparticles significantly increased the fracture toughness of the material, which fitted the ISO standard classification as a “Class 2” ceramic.

As for the data from the flexural strength test, although the addition of nanoparticles has reduced the flexural strength of material, the values still allow it to adhere to ISO standard as a “Class 2” ceramic as well. Additionally, it is important to highlight that there was no significant difference between the Weibull modulus of the materials, which indicates reliability (low variability and similar failure probability). For the same group, the characteristics of the materials are very similar, which led them to behave in a similar way.

The ISO 6872 determines the level of accepted solubility of both directly (“enamel”) and indirectly (“core”) exposed dental ceramics to the oral environment. Enamel class dental ceramics should display up to 100 μg/cm^2 for maximum solubility level, whereas core class ceramics must show less than 2000 μg/cm^2. Unfortunately, however, none of the experimental materials chemical solubility could achieve an acceptable chemical solubility value (> 2000 μg/cm^2). The SEM analysis of pre- and post-solubility testing for all tested materials in this research provided visible evidence that the experimental ceramics’ surfaces were affected when subjected to a corrosive environment, with a very high degree of effect, exceeding the allowed limit.

Hawsawi et al. 2020 [12] proved that geometry and size of individual specimen can affect the solubility test outcomes. Specimens containing a geometry of edges and corners and with a small individual surface were more damaged and had increased in

solubility. Furthermore, by analyzing the literature, there are only a few published studies regarding dental ceramics' chemical solubility that have adhered to the method described in the ISO 6872. This may indicate a possible lack of confidence of the ISO standard method.

This is the first study that evaluates the chemical solubility of a calcium phosphate ceramic according to the recommendations of ISO 6872:2015 for dental use. Therefore, this material requires more investigations.

5. CONCLUSION

The experimental calcium phosphate ceramic with additions of 5% and 8% of TiO_2 achieved desirable mechanical properties, but the chemical solubility values did not allow it to become a dental ceramic.

REFERENCES

[1] Eliaz N, Metoki N. Calcium phosphate bioceramics: a review of their history, structure, properties, coating technologies and biomedical applications. Materials (Basel) 2017; 10(4):334. https://doi.org/10.3390/ma10040334

[2] Ibrahim M, Labaki M, Giraudon JM, Lamonier JF. Hydroxyapatite, a multifunctional material for air, water and soil pollution control: a review. J Hazard Mater 2020; 383:121139. https://doi.org/10.1016/j.jhazmat.2019.121139

[3] Ghiasi B, Sefidbakht Y, Mozaffari-Jovin S, Gharehcheloo B, Mehrarya M, Khodadadi A et al. Hydroxyapatite as a biomaterial - a gift that keeps on giving. Drug Dev Ind Pharm 2020; 46(7):1035-62. https://doi.org/10.1080/03639045.2020.1776321

[4] Prakasam M, Locs J, Salma-Ancane K, Loca D, Largeteau A, Berzina-Cimdina L. Fabrication, properties and applications of dense hydroxyapatite: a review. J Funct Biomater 2015; 6(4):1099-140. https://doi.org/10.3390/jfb6041099

[5] Mbarki M, Sharrock P, Fiallo M, ElFeki H. Hydroxyapatite bioceramic with large porosity. Mater Sci Eng C Mater Biol Appl 2017; 76:985-90. https://doi.org/10.1016/j.msec.2017.03.097

[6] Pires LA, de Azevedo Silva LJ, Ferrairo BM, Erbereli R, Lovo JFP, Ponce Gomes O et al. Effects of ZnO/TiO2 nanoparticle and TiO2 nanotube additions to dense polycrystalline hydroxyapatite bioceramic from bovine bones. Dent Mater 2020; 36(2):e38-e46. https://doi.org/10.1016/j.dental.2019.11.006

[7] Bordea IR, Candrea S, Alexescu GT, Bran S, Băciuț M, Băciuț G et al. Nano-hydroxyapatite use in dentistry: a systematic review. Drug Metab Rev 2020; 52(2):319-32. https://doi.org/10.1080/03602532.2020.1758713

[8] Akram M, Ahmed R, Shakir I, Ibrahim WAW, Hussain R. Extracting hydroxyapatite and its precursors from natural resources. J Mater Sci 2014; 49:1461-75. https://doi.org/10.1007/s10853-013-7864-x

[9] Mohd Pu'ad NAS, Koshy P, Abdullah HZ, Idris MI, Lee TC. Syntheses of hydroxyapatite from natural sources. Heliyon 2019; 5(5):e01588. https://doi.org/10.1016/j.heliyon.2019.e01588

[10] Agbeboh NI, Oladele IO, Daramola OO, Adediran AA, Olasukanmi OO, Tanimola MO. Environmentally sustainable processes for the synthesis of hydroxyapatite. Heliyon 2020; 6(4):e03765. https://doi.org/10.1016/j.heliyon.2020.e03765

[11] Baino F, Novajra G, Vitale-Brovarone C. Bioceramics and scaffolds: a winning combination for tissue engineering. Front Bioeng Biotechnol 2015; 3:202. https://doi.org/10.3389/fbioe.2015.00202

[12] Hawsawi RA, Miller CA, Moorehead RD, Stokes CW. Evaluation of reproducibility of the chemical solubility of dental ceramics using ISO 6872:2015. J Prosthet Dent 2020; 124(2):230-6. https://doi.org/10.1016/j.prosdent.2019.09.016

[13] British Standards Institution. BS ISO 6872: dentistry e ceramic materials. London: BSI; 2015.

[14] Faber KT, Evans AG. Crack deflection processes-I. Theory. Acta Metall 1983; 31(4):565–76. https://doi.org/10.1016/0001-6160(83)90046-9

[15] Fathi HM, Miller C, Stokes C, Johnson A. The effect of ZrO2 and TiO2 on solubility and strength of apatite-mullite glass-ceramics for dental applications. J Mater Sci Mater Med 2014; 25(3):583-94. https://doi.org/10.1007/s10856-013-5096-x

[16] Wetzel B, Rosso P, Haupert F, Friedrich K. Epoxy nanocomposites–fracture and toughening mechanisms. Eng Fract Mech 2006; 73(16):2375-98. https://doi.org/10.1016/j.engfracmech.2006.05.018

[17] Xia Y, Zhang F, Xie H, Gu N. Nanoparticle-reinforced resin-based dental composites. J Dent 2008; 36(6):450-5. https://doi.org/10.1016/j.jdent.2008.03.001

[18] Ghahremani L, Shirkavand S, Akbari F, Sabzikari N. Tensile strength and impact strength of color modified acrylic resin reinforced with titanium dioxide nanoparticles. J Clin Exp Dent 2017; 9(5):e661-e665. https://dx.doi.org/10.4317/jced.53620

[19] Elsaka SE, Hamouda IM, Swain MV. Titanium dioxide nanoparticles addition to a conventional glass-ionomer restorative: influence on physical and antibacterial properties. J Dent 2011; 39(9):589-98. https://doi.org/10.1016/j.jdent.2011.05.006

[20] Sodagar A, Akhoundi MSA, Bahador A, Jalali YF, Behzadi Z, Elhaminejad F et al. Effect of TiO2 nanoparticles incorporation on antibacterial properties and shear bond strength of dental composite used in Orthodontics. Dental Press J Orthod 2017; 22(5):67-74. https://doi.org/10.1590/2177-6709.22.5.067-074.oar

[21] Gracis S, Thompson VP, Ferencz JL, Silva NR, Bonfante EA. A new classification system for all-ceramic and ceramic-like restorative materials. Int J Prosthodont 2015; 28(3):227-35. https://doi.org/10.11607/ijp.4244

[22] Ponton CB, Rawlings RD. Vickers indentation fracture toughness test Part 1 Review of literature and formulation of standardised indentation toughness equations. Mater Sci and Techol 1989; 5(9):865–72. https://doi.org/10.1179/mst.1989.5.9.865

[23] Gupta SM, Tripathi MA. Review of TiO2 nanoparticles. Chin Sci Bull (2011); 56. https://doi.org/10.1007/s11434-011-4476-1

[24] Catauro M, Tranquillo E, Dal Poggetto G, Pasquali M, Dell'Era A, Vecchio Ciprioti S. Influence of the heat treatment on the particles size and on the crystalline phase of tio_2 synthesized by the sol-gel method. Materials (Basel) 2018; 11(12):2364. https://doi.org/10.3390/ma11122364

[25] Kusrini E, Sontang M. Characterization of x-ray diffraction and electron spin resonance: effects of sintering time and temperature on bovine hydroxyapatite. Radiat Phys Chem 2012; 81(2):118-25. https://doi.org/10.1016/j.radphyschem.2011.10.006

[26] Rincón-López JA, Hermann-Muñoz JA, Giraldo-Betancur AL, De Vizcaya-Ruiz A, Alvarado-Orozco JM, Muñoz-Saldaña J. Synthesis, characterization and in vitro study of synthetic and bovine-derived hydroxyapatite ceramics: a comparison. Materials (Basel) 2018; 11(3):333. https://doi.org/10.3390/ma11030333

[27] Champion E. Sintering of calcium phosphate bioceramics. Acta Biomater 2013; 9(4):5855-75. https://doi.org/10.1016/j.actbio.2012.11.029

[28] Orlovskii VP, Komlev VS, Barinov SM. Hydroxyapatite and hydroxyapatite-based ceramics. Inorg Mater 2002; 38(10):973–84. https://doi.org/10.1023/A:1020585800572

[29] Salma, K., Berzina-Cimdina, L., Borodajenko, N. Calcium phosphate bioceramics prepared from wet chemically precipitated powders. Process Appl Ceram 2010; 4(1):45–51. https://doi.org/10.2298/PAC1001045S

[30] Malina D, Bertnat K, Sobczak-Kupiec A. Studies on sintering process of synthetic hydroxyapatite. Acta Biochim Pol 2013; 60(4). https://doi.org/10.18388/abp.2013_2071

[31] Indurkar A, Choudhary R, Rubenis K, Locs J. Advances in sintering techniques for calcium phosphates ceramics. Materials (Basel) 2021; 14(20):6133. https://doi.org/10.3390/ma14206133

REFERÊNCIAS

AGBEBOH, N. I. *et al.* Environmentally sustainable processes for the synthesis of hydroxyapatite. **Heliyon**, London, v. 6, n. 4, e03765, Apr. 2020. DOI: 10.1016/j.heliyon.2020.e03765. Disponível em: https://www.ncbi.nlm.nih.gov/pmc/articles/PMC7184159/pdf/main.pdf. Acesso em: 17 maio 2022.

AKRAM, M. *et al.* Extracting hydroxyapatite and its precursors from natural resources. **J Mater Sci**, New York, v. 49, n. 4, p. 1461-1475, 2014. DOI: 10.1007/s10853-013-7864-x. Disponível em: https://link.springer.com/content/pdf/10.1007/s10853-013-7864-x.pdf. Acesso em: 17 maio 2022.

BORDEA, I. R. *et al.* Nano-hydroxyapatite use in dentistry: a systematic review. **Drug Metab Rev**, New York, v. 52, n. 2, p. 319-332, May 2020. DOI: 10.1080/03602532.2020.1758713. Disponível em: https://www.researchgate.net/profile/Adina-Todea/publication/341325072_Nano-hydroxyapatite_use_in_dentistry_a_systematic_review/links/5f1f0144a6fdcc9626b6ec7b/Nano-hydroxyapatite-use-in-dentistry-a-systematic-review.pdf. Acesso em: 17 maio 2022.

ELIAZ, N.; METOKI, N. Calcium phosphate bioceramics: a review of their history, structure, properties, coating technologies and biomedical applications. **Materials**, Basel, v. 10, n. 4, p. 334, Mar. 2017. DOI: 10.3390/ma10040334. Disponível em: https://www.ncbi.nlm.nih.gov/pmc/articles/PMC5506916/pdf/materials-10-00334.pdf. Acesso em: 17 maio 2022.

ELSAKA, S. E.; HAMOUDA, I. M.; SWAIN, M. V. Titanium dioxide nanoparticles addition to a conventional glass-ionomer restorative: influence on physical and antibacterial properties. **J Dent**, Bristol, v. 39, n. 9, p. 589-598, Sept. 2011. DOI: 10.1016/j.jdent.2011.05.006. Disponível em: https://www.sciencedirect.com/science/article/pii/S030057121100128X?via%3Dihub. Acesso em: 17 maio 2022.

FABER, K. T.; EVANS, A. G. Crack deflection processes – part I. Theory. **Acta Metall,** Kidlington, v. 31, n. 4, p. 565–576, Apr. 1983. DOI: 10.1016/0001-6160(83)90046-9. Disponível em: https://doi.org/10.1016/0001-6160(83)90046-9. Acesso em: 17 maio 2022.

FATHI, H. M. *et al*. The effect of ZrO2 and TiO2 on solubility and strength of apatite-mullite glass-ceramics for dental applications. **J Mater Sci Mater Med**, London, v. 25, n. 3, p. 583-594, Mar. 2014. DOI: 10.1007/s10856-013-5096-x. Disponível em: https://link.springer.com/content/pdf/10.1007/s10856-013-5096-x.pdf. Acesso em: 17 maio 2022.

GHAHREMANI, L. *et al*. Tensile strength and impact strength of color modified acrylic resin reinforced with titanium dioxide nanoparticles. **J Clin Exp Dent,** [Spain], v. 9, n.5, e661-e665, May 2017. DOI: 10.4317/jced.53620. Disponível em: https://www.ncbi.nlm.nih.gov/pmc/articles/PMC5429478/pdf/jced-9-e661.pdf. Acesso em: 17 maio 2022.

GHIASI, B. *et al*. Hydroxyapatite as a biomaterial - a gift that keeps on giving. **Drug Dev Ind Pharm,** New York, v. 46, n. 7, p. 1035-1062, July 2020. DOI:

10.1080/03639045.2020.1776321. Disponível em: https://www.tandfonline.com/doi/abs/10.1080/03639045.2020.1776321?journalCode=iddi20. Acesso em: 17 maio 2022.

GRACIS, S. *et al*. A new classification system for all-ceramic and ceramic-like restorative materials. **Int J Prosthodont**, Lombard, v. 28, n. 3, p. 227-235, May/June 2015. DOI: 10.11607/ijp.4244. Disponível em: http://quintpub.com/journals/ijp/full_txt_pdf_alert.php?article_id=15276. Acesso em: 17 maio 2022.

HAWSAWI, R. A. *et al*. Evaluation of reproducibility of the chemical solubility of dental ceramics using ISO 6872:2015. **J Prosthet Dent**, St. Louis, v. 124, n. 2, p. 230-236, Aug. 2020. DOI: 10.1016/j.prosdent.2019.09.016. Disponível em: https://www.sciencedirect.com/science/article/pii/S0022391319306080?via%3Dihub. Acesso em: 17 maio 2022.

ISO - International Organization for Standardization. **ISO/BS 6872:2015**: dentistry: ceramic materials. London: ISO, 2015. 28p.

JAYATHILAKAN, K. *et al*. Utilization of byproducts and waste materials from meat, poultry and fish processing industries: a review. **J Food Sci Technol**, Mysore, v. 49, n. 3, p. 278-293, June 2012. DOI: 10.1007/s13197-011-0290-7. Disponível em: https://www.ncbi.nlm.nih.gov/pmc/articles/PMC3614052/pdf/13197_2011_Article_290.pdf. Acesso em: 17 maio 2022.

KUSRINI, E.; SONTANG, M. Characterization of x-ray diffraction and electron spin resonance: effects of sintering time and temperature on bovine hydroxyapatite. **Radiat Phys Chem**, Oxford, v. 81, n. 2, p. 118-125, Feb. 2012. DOI: 10.1016/j.radphyschem.2011.10.006. Disponível em: https://doi.org/10.1016/j.radphyschem.2011.10.006. Acesso em: 17 maio 2022.

LIM, K. T. *et al*. Human teeth-derived bioceramics for improved bone regeneration. **Nanomaterials**, Basel, v. 10, n. 12, p. 2396, Nov. 2020. DOI: 10.3390/nano10122396. Disponível em: https://www.ncbi.nlm.nih.gov/pmc/articles/PMC7761315/pdf/nanomaterials-10-02396.pdf. Acesso em: 17 maio 2022.

MBARKI, M. *et al*. Hydroxyapatite bioceramic with large porosity. **Mater Sci Eng C Mater Biol Appl**, Amsterdam, v. 76, p. 985-990, July 2017. DOI: 10.1016/j.msec.2017.03.097. Disponível em: https://doi.org/10.1016/j.msec.2017.03.097. Acesso em: 17 maio 2022.

MOHD PU'AD, N. A. S. *et al*. Syntheses of hydroxyapatite from natural sources. **Heliyon**, London, v. 5, n. 5, e01588, May 2019. DOI: 10.1016/j.heliyon.2019.e01588. Disponível em: https://www.ncbi.nlm.nih.gov/pmc/articles/ PMC6507053/pdf/main.pdf. Acesso em: 17 maio 2022.

MONROE, E. A. *et al*. New calcium phosphate ceramic material for bone and tooth implants. **J Dent Res**, Chicago, v. 50, n. 4, p. 860-861, July/Aug. 1971. DOI: 10.1177/00220345710500041201. Disponível em: https://doi.org/10.1177/00220345710500041201. Acesso em: 17 maio 2022.

PIRES, L. A. *et al*. Effects of ZnO/TiO2 nanoparticle and TiO2 nanotube additions to dense polycrystalline hydroxyapatite bioceramic from bovine bones. **Dent Mater**, Copenhagen, v. 36, n. 2, e38-e46, Feb. 2020. DOI: 10.1016/j.dental.2019.11.006. Disponível em: https://doi.org/10.1016/j.dental.2019.11.006. Acesso em: 17 maio 2022.

POGGIO, C. E. *et al*. Metal-free materials for fixed prosthodontic restorations. **Cochrane Database Syst Rev**, Oxford, v. 12, n. 12, CD009606, Dec. 2017. DOI: 10.1002/14651858.CD009606.pub2. Disponível em: https://www.ncbi.nlm.nih.gov/pmc/articles/PMC6486204/pdf/CD009606.pdf. Acesso em: 17 maio 2022.

PRAKASAM, M. *et al*. Fabrication, properties and applications of dense hydroxyapatite: a review. **J Funct Biomater**, Basel, v. 6, n. 4, p. 1099-1140, Dec. 2015. DOI: 10.3390/jfb6041099. Disponível em: https://www.ncbi.nlm.nih.gov/pmc/articles/PMC4695913/pdf/jfb-06-01099.pdf. Acesso em: 17 maio 2022.

RINCÓN-LÓPEZ, J. A. *et al.* Synthesis, characterization and in vitro study of synthetic and bovine-derived hydroxyapatite ceramics: a comparison. **Materials**, Basel, v. 11, n. 3, p. 333, Feb. 2018. DOI: 10.3390/ma11030333. Disponível em: https://www.ncbi.nlm.nih.gov/pmc/articles/PMC5872912/pdf/materials-11-00333.pdf. Acesso em: 17 maio 2022.

SODAGAR, A. *et al*. Effect of TiO2 nanoparticles incorporation on antibacterial properties and shear bond strength of dental composite used in Orthodontics. **Dental Press J Orthod,** Maringá, v. 22, n. 5, p. 67-74, Sept./Oct. 2017. DOI: 10.1590/2177-6709.22.5.067-074.oar. Disponível em: https://www.ncbi.nlm.nih.gov/pmc/articles/PMC5730138/pdf/2176-9451-dpjo-22-05-00067.pdf. Acesso em: 17 maio 2022.

SWETHA, M. *et al*. Biocomposites containing natural polymers and hydroxyapatite for bone tissue engineering. **Int J Biol Macromol**, Guildford, v. 47, n. 1, p. 1-4, July 2010. DOI: 10.1016/j.ijbiomac.2010.03.015. Disponível em: https://doi.org/10.1016/j.ijbiomac.2010.03.015. Acesso em: 17 maio 2022.

XIA, Y. *et al*. Nanoparticle-reinforced resin-based dental composites. **J Dent**, Bristol, v. 36, n. 6, p. 450-455, June 2008. DOI: 10.1016/j.jdent.2008.03.001. Disponível em: https://doi.org/10.1016/j.jdent.2008.03.001. Acesso em: 17 maio 2022.

WETZEL, B. *et al*. Epoxy nanocomposites – fracture and toughening mechanisms. **Eng Fract Mech**, New York, v. 73, n. 16, p. 2375-2398, Nov. 2006. DOI: 10.1016/j.engfracmech.2006.05.018. Disponível em: https://doi.org/10.1016/j.engfracmech.2006.05.018. Acesso em: 17 maio 2022.